CHAPTER 1

Analysis of Common Mode Inductors and Optimization Aspects

Anne Roc'h[1,*] and Frank Leferink[1,2]

[1]Department of Telecommunication Engineering, University of Twente, Drienerlolaan 5, 7522 NB Enschede, The Netherlands and [2]Thales Nederland, Hengelo, Haaksbergerstraat 49, 7554 PA Hengelo, The Netherlands.

Abstract: The common mode inductors, or common mode chokes, are a key component of electromagnetic interference filters. Engineers usually face significant design challenges such as size, cost and weight while working with these components. To avoid the construction of several prototypes, often oversized, engineers need an analytical method to predict performances of the filter. The analysis of the common mode inductors starts with a presentation of the different ferromagnetic materials: their properties are the cornerstone of the design of the component. Based on this study, the impedances used to characterize the choke are related to the designable parameters. The derived model shows the role of the parasitic currents to ground and the common mode impedance in the overall common mode current attenuation. A certain attenuation of differential mode current is also to be expected due to the parasitic currents of the common mode choke itself: the turn to turn capacitance and the leakage inductance. This model is validated by measurements. Sensitivity studies provide an additional insight into the behavior of the choke by giving an understanding on how variations of parameters, influence the final performance. The deviation calculation and the influence of the designable parameters are addressed at the end of this chapter.

Keywords: Capacitive coupling, Common mode current, Core material, Curie temperature, Differential mode current, Electromagnetic interference (EMI), Equivalent circuit, Ferromagnetic material, Ferromagnetism, Flux, Ferrite, Filter, Hysteresis loop, Heat, Inductance, Impedance, Iron, Modification factors, Metal alloys, Noise source, Nanocrystalline, Noise spectrum, Powder material, Permeability, Power converter, Radiated electric field, Saturation level, Sensitivity.

INTRODUCTION

Power electronic converters consist of a switching devices which are turned on or off, based on a modulation technique to adjust output voltage and/or frequency. They can be classified as AC-to-DC, DC-to-DC, DC-to-AC and AC-to-AC [1]. Fig. **1** contains a general presentation of the structure of frequency converters. They have a main drawback: the high level of electromagnetic interferences (EMI) generated on power lines and motor cables, due to the non-ideal behaviour of the switches. The noise spectrum is usually spread from around 10 kHz to several decades of MHz. Filtering the main supply and motor cables adequately is a challenge which often leads to retro-designed filters, tested in a 'cut and try' process [2], [3], [4]. Design constraints as size, cost and weight are common while working with such components. Availability of analytical methods to predict performances of the filters would reduce or avoid the need for construction of several, often oversized, prototypes.

Common mode (CM) currents are frequently referred at 'antenna-mode' currents and are the predominant mechanism for producing radiated electric field in practical products [5]. Fig. **3** presents the circulation of common mode current in a motor drive. These currents usually flow along the cable and return to the source *via* stray capacitances between the cable and the ground and to certain extent *via* capacitive coupling between the frame of the motor and the ground.

Passive filtering of common mode currents involves a combination of capacitors and common mode chokes because the value of the capacitance to ground is limited. The common mode choke is a key element in terms of performances, size, cost and weight of the overall filter and is the focus of this chapter.

The two following examples show the impact of the common mode filter on the level of electromagnetic interferences: Fig. **1** presents the attenuation of current at the output of a common-mode filter used in an AC/DC converter in which a MnZn ferrite of 10 mH is used in combination with two feed through Y-capacitors. The impact

***Address correspondence to Anne Roc'h:** Department of Telecommunication Engineering, University of Twente, Drienerlolaan 5, 7522 NB Enschede, The Netherlands; E-mail: anne.roch@gmail.com

Firuz Zare (Ed)
All rights reserved - © 2011 Bentham Science Publishers

of a common mode filter on the level of radiated emission between 10kHz and 1GHz is shown in Fig. **2**. This filter has been built with nanocrystalline cores and constitutes a good example of an alternative design to the classical iron choke solution which will be detailed in this chapter. Designs of both these filters are detailed in [3] and [6].

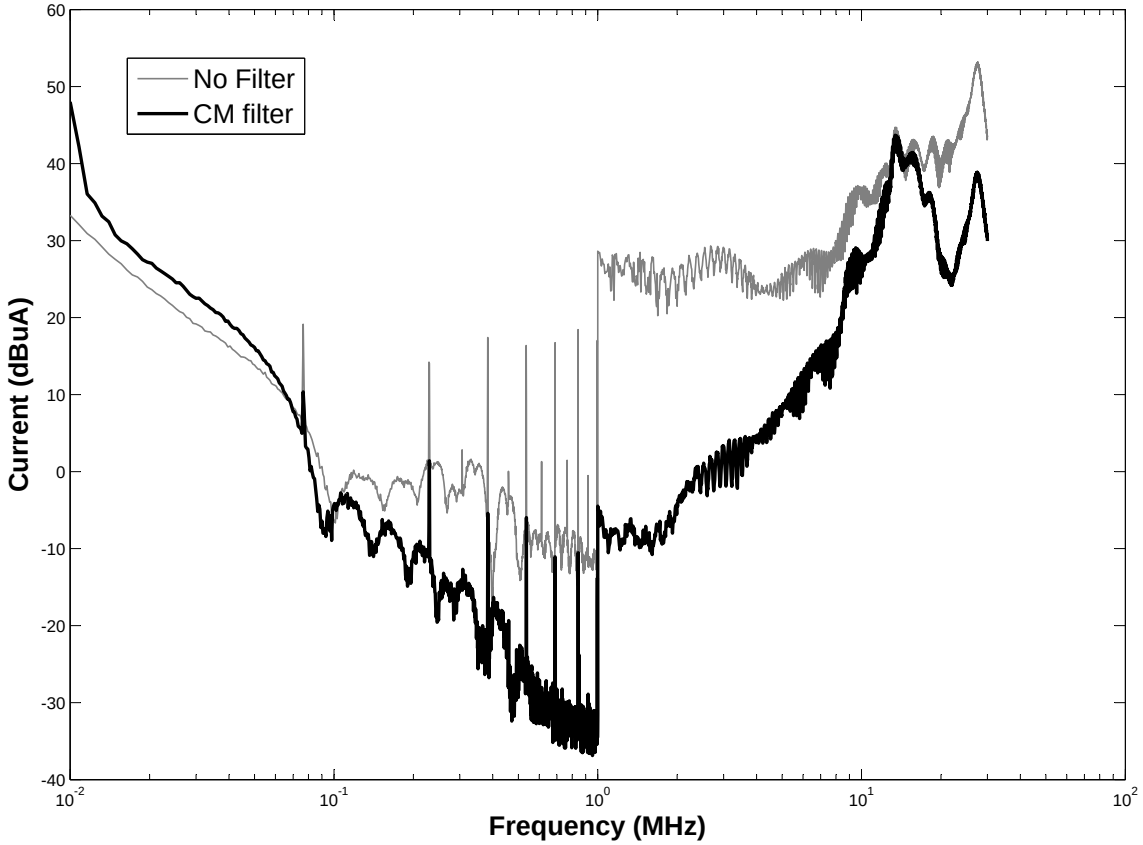

Figure 1: Input common mode current attenuation of an input filter of an AC/DC converter from 10kHz to 30MHz (level in dBµA).

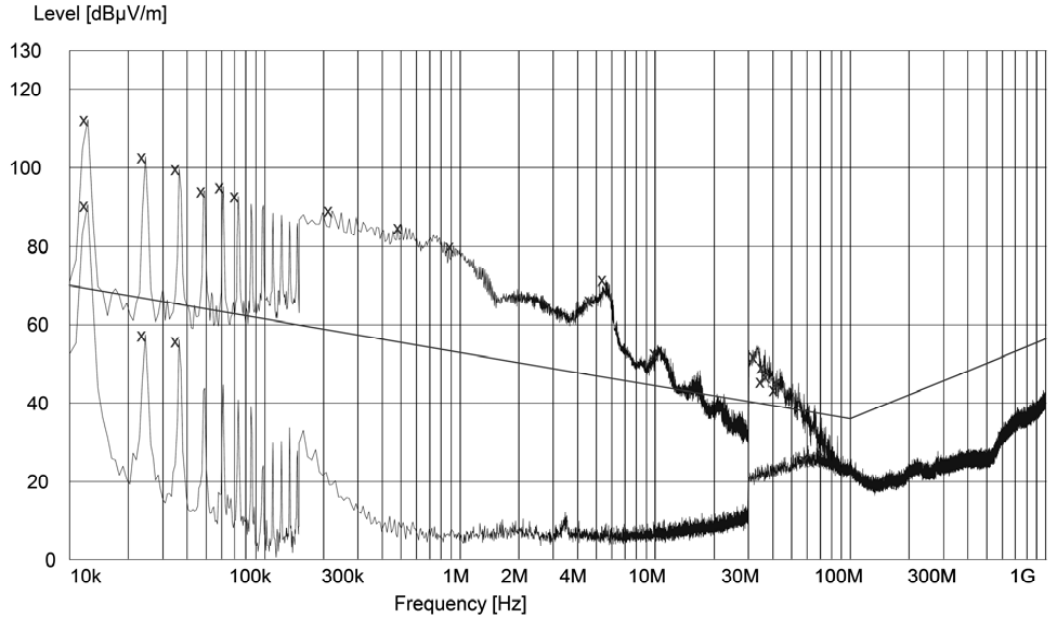

Figure 2: Radiated emission attenuation of an output filter for frequency converter from 10kHz to 1GHz (Level in dBµV/m).

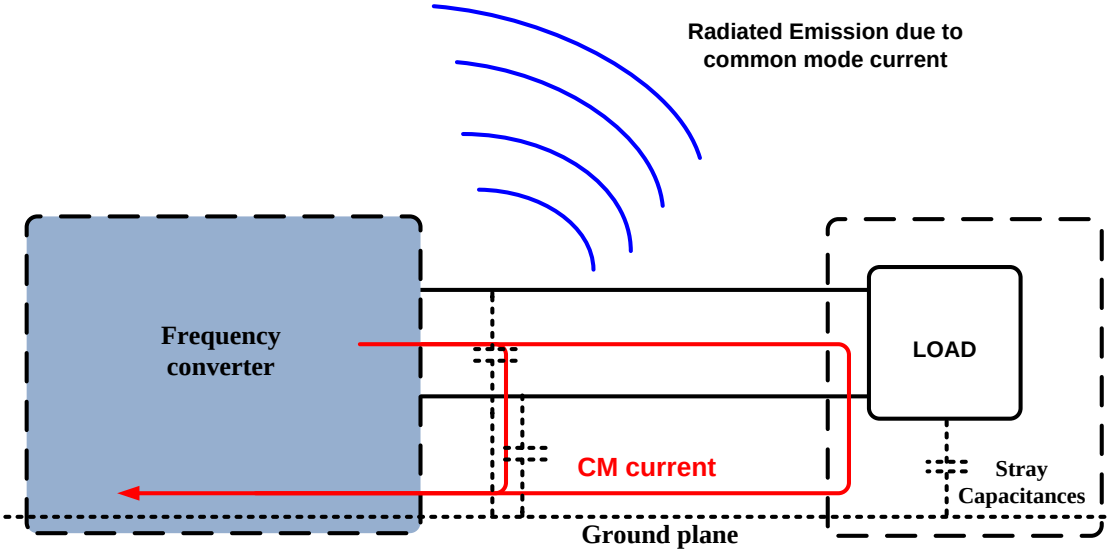

Figure 3: The common mode current path in a motor drive.

CORE MATERIALS

The core material can be used to increase the inductance, or to absorb energy and to transformed it in heat. The main purpose of a CM choke is not for energy storage but it is for a transformation of this energy to heat. The amount of common mode current that will be transform in heat by the common mode choke and the frequency range of efficiency will be first determined by the material itself and then by the overall design.

Ferromagnetic materials are typically used: iron powder material, ferrites, meta-materials and nanocrystalline. In this section the general material properties are first reviewed. The levels of permeability and saturation as well as the Curie temperature of materials are compared with each other.

Core Material Properties: Overview

Ferromagnetism. In a ferromagnetic material there is parallel alignment of the atomic moment in a domain. Each domain thus becomes a magnet. Their size and geometry are formed to reduce the magnetic potential contained in the field lines connecting north to south outside the material. Each domain contains about 10^{15} atoms. In this condition the magnetic flux path never leaves the boundary of the material. The region where the magnetization is the same, is called a 'domain wall'. When an electromagnetic flux is created across a ferromagnetic material the domains become aligned to produce a strong magnetic field within the part. Electromagnetic energy is transferred to the core which stored or transformed into heat depending on the frequency. The main purpose of a common mode choke though is not for energy storage but for the transformation of this energy into heat.

Permeability. In order to evaluate the total flux density in a ferromagnetic material it is useful to define the permeability μ which is the ratio of the magnetic flux density B, to magnetizing field H. It is the most important parameter used to characterize a magnetic material. The relative permeability μ_r is the ratio of the permeability μ *to* μ_o, where $\mu_o=4.\pi*10^{-7}\ H.m^{-1}$ is the permeability of free space.

The common mode choke is used for its core loss properties that are related to the imaginary part of the complex permeability and less for its inductive properties (related to the real part of the complex permeability).

Hysteresis loop and saturation level. Presentation. As the current goes through one sine-wave cycle, the magnetization goes through one hysteresis loop cycle. Minor hysteresis loops are obtained when the maximum applied field is lower than that required to saturate the material. Fig. **4** presents the shape of a hysteresis loop in a ferromagnetic material.

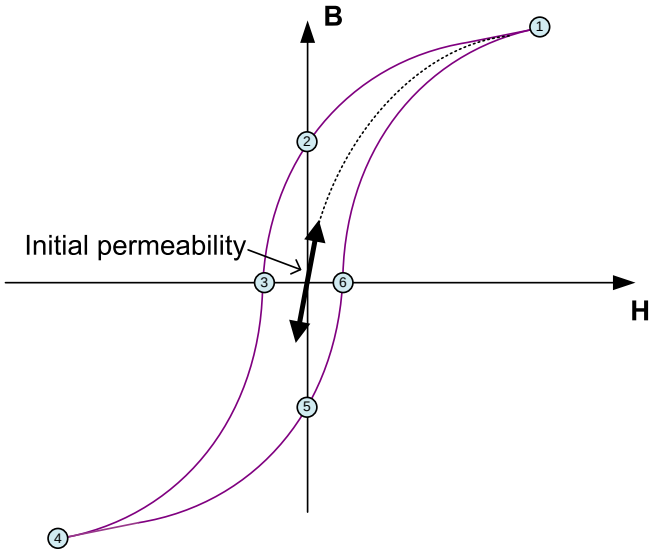

Figure 4: Hysteresis loop in a ferromagnetic material.

Hysteresis loop modeling. Permeability of the material is the slope of the *BH* loop and reduces close to the saturation. At this stage the common mode choke will not absorb energy anymore, and the common mode impedance is low. For these two reasons it is important for the designer to have knowledge about the shape of the *B-H*-loop.

Several approaches [13] have been developed to predict the major *B-H* loop of ferrites. In particular the Jiles-Atherton model [14] is convenient. It comprises of a first order non-linear differential equation which can be solved numerically to give the magnetization *M*, as a function of the applied magnetic field *H*.

The *B-H* loop is dependent of the topology of the cores and the main drawback of this method in a predictive model which is the need of experimental extraction of the so-called 'Jiles Atherton parameters' on the common mode choke itself. A solution is to combine the Jiles-Atherton model with the extraction parameters algorithm as described in [17].

Hysteresis loop in transient condition. The hysteresis loop as described in the previous section and its related Jiles-Atherton model are valid only when the current goes through a sine-wave cycle. In [15] the concept of volume fraction is introduced to model hysteresis loop of ferrite cores excited by a transient magnetic field. The Jiles-Atherton model is modified in a loop by loop technique in order to obtain the magnetization trajectory with an asymmetric minor loop excursion under arbitrary waveform magnetic field excitation. This technique is specially developed for power transformers and chokes used in power electronics converters. For high frequency operation (above 400 Hz) an additional technique has to be incorporated in this model to deal with rate of dependent hysteresis effect NL Mi, Oruganti R, SX Chen. Modeling of hysteresis loops of ferrite cores excited by a transient magnetic field Magnetics, IEEE Trans 1998; 34(4): 1294-1296

[16]. The hysteresis loop does indeed enlarge as the frequency increases and the permeability on the other hand decreases.

These models in transient conditions remain experimental: for each core and each wiring system tested on this core, five experimental parameters have to be initially extracted. This is due to the structure of the Jiles-Atherton model. They are useful for an accurate prediction of waveforms and hysteresis losses in a time domain.

Choke materials belong to the soft magnetic material family and are characterized by a narrower *B-H* loop. For low power application and/or in a choke used relatively far from its saturation condition, the permeability (slope coefficient of the hysteresis loop) remains similar to the initial permeability. The initial permeability is the parameter usually provided by manufacturer.

Curie temperature. The spontaneous magnetization of ferromagnetic material disappears at the Curie temperature. It is then important to ensure that the temperature of the choke remains below this temperature.

General Material Overview

The typical requirements of an optimized common mode choke are:

- A high impedance over the wanted frequency-range, this is related to the complex permeability of the material,
- A high saturation level,

Three basic materials: ferrites, powder materials (iron) and metal alloys (nanocrystalline and amorphous structure), are used in the design of the traditional common mode choke for switched mode power supplies (SMPS). Fig. **5** presents a synthetic overview of the permeability of nanocrystalline, ferrites, iron and amorphous materials [20-23].

The highest initial permeabilities are found in nanocrystalline materials (up to 10 000 till 150 kHz). Iron powder cores have low permeabilities (10 to 100 till 100 kHz) while amorphous alloys have higher values (5000 to 80 000 till 100 kHz). Ferrite cores can be used over a wide frequency range (up to several MHz for the NiZn cores). Higher flux density can be found in nanocrystalline and amorphous material, as well as in iron powder core. Ferrites exhibit a significantly lower level of saturation; this is depicted in Fig. **6**.

Iron based nanocrystalline materials are the new generation of magnetic alloys. Typical characteristic of these materials is their small nanometer grain size. Concept of nanocrystalline materials was introduced in 1981 [25]. Research on this new material has progressed after the development of the first nanocrystalline material in 1988.

Nanocrystalline materials are a good alternative to the traditional chokes made of ferrite or iron powder: the main advantage of this material is its high levels of saturation and in its relatively smaller size, it is however more expensive than the other materials. This newer material is a major step towards volume reduction, reaching 50-80% lower compared to a ferrite core and more than 90% lower compared to an iron core. The consequent weight loss can be an important property in aerospace applications or any other area where weight is a design constraint.

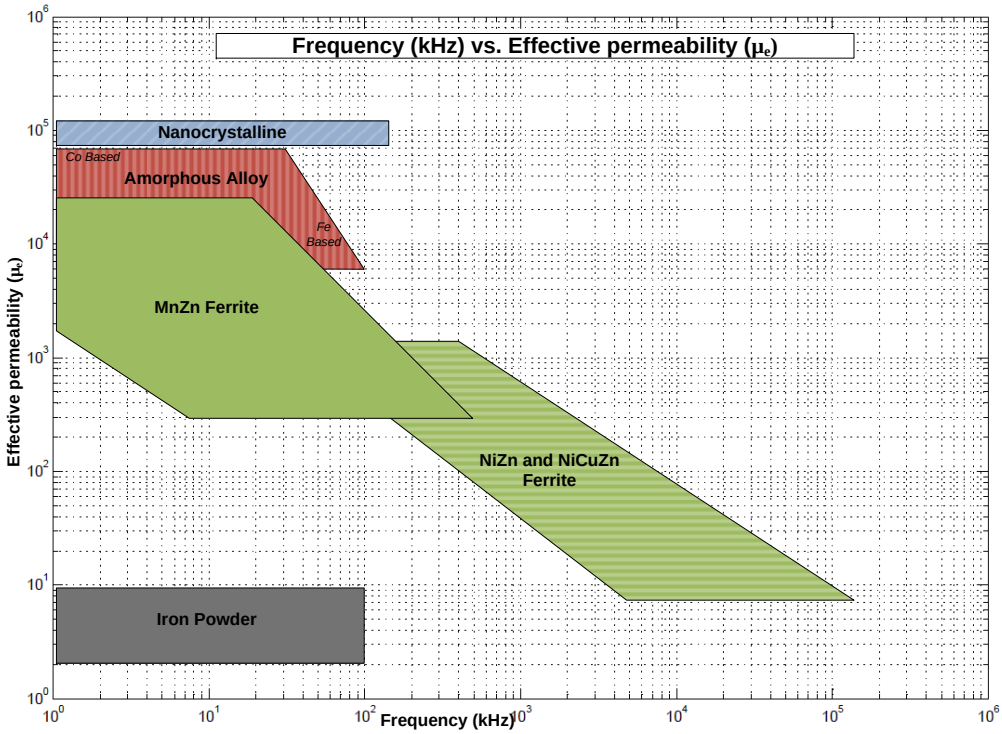

Figure 5: Main magnetic properties for the material ferrites, nanocrystalline and amorphous: Permeability vs. Frequency.

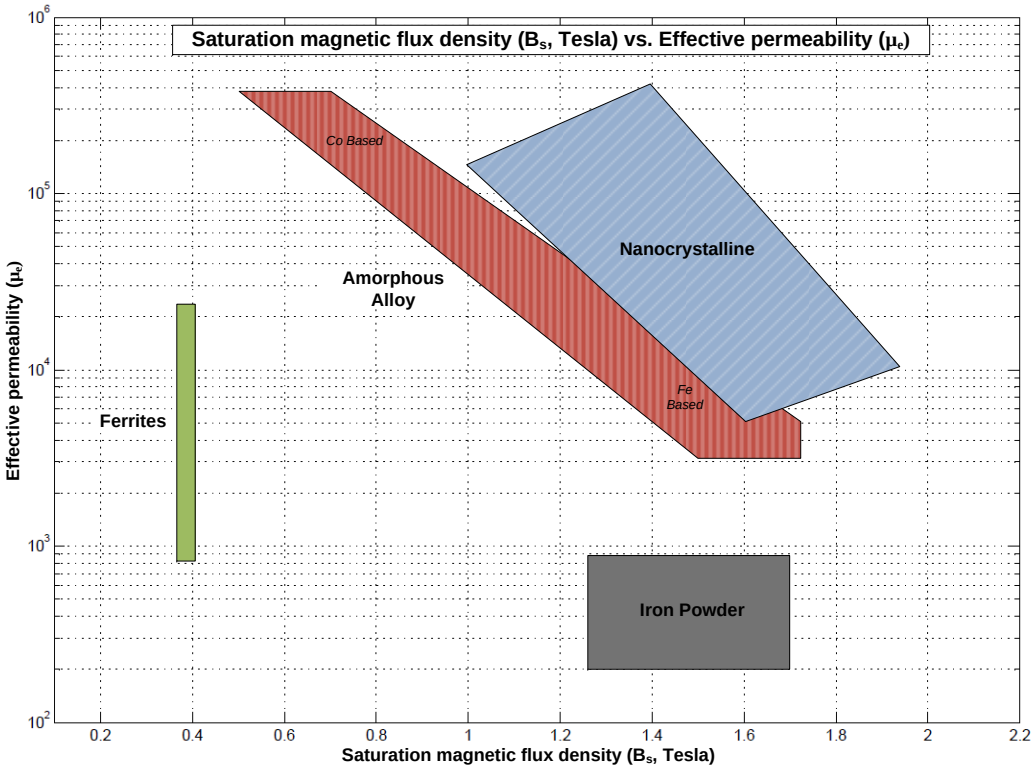

Figure 6: Main magnetic properties for the material ferrites, nanocrystalline and amorphous: Saturation vs. permeability.

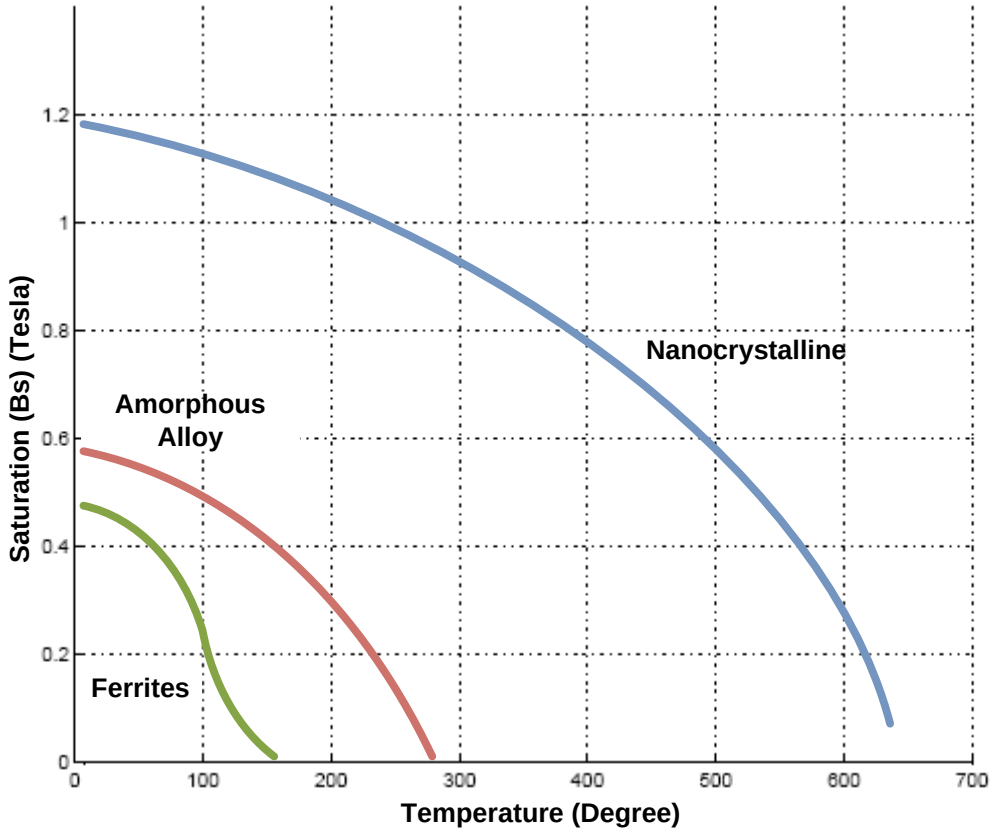

Figure 7: Temperature vs. Saturation.

Iron remains however the lowest cost option of the four family of materials. An equivalent ferrite solution would be about 4 times more expensive. A nanocrystalline or an amorphous solution would be between 7 and 10 times more costly than an iron solution [24]. Fig. **7** presents the evolution of the saturation level with the Curie temperature.

COMMON MODE CHOKES, IMPEDANCES AND DESIGNABLE PARAMETERS

This section focuses on the designable parameters of the common mode choke (CMC) and their related impedance modeling.

Common Mode Chokes Presentation

A main objective of a common mode choke is to block the emission noise (electromagnetic interferences) while the lower frequency range of the signals are not affected. Common mode inductors are wound with two or three windings of equal numbers of turns. The number of windings is same as the number of phases. As depicted in Fig. **8**, the windings are placed on the core so that the line currents in each winding create fluxes that are equal in magnitude but opposite in phase in the case of differential currents, and identical in the case of common mode currents. The fluxes of the differential mode currents are thus ideally cancelling out each other and the related current is not influenced by the inductors. It will be shown later that the cancellation of the fluxes cannot be achieved completely. The fluxes due to the common mode currents are in the same direction. These currents go together through equivalent common mode impedance related to the material properties and are transformed into heat.

Impedances and Designable Parameters Identification

The designable parameters are the quantitative aspects of physical characteristics of the common mode choke that are input to its design process. In this section the designable parameters of a common mode choke are related to their impedances in its equivalent circuit.

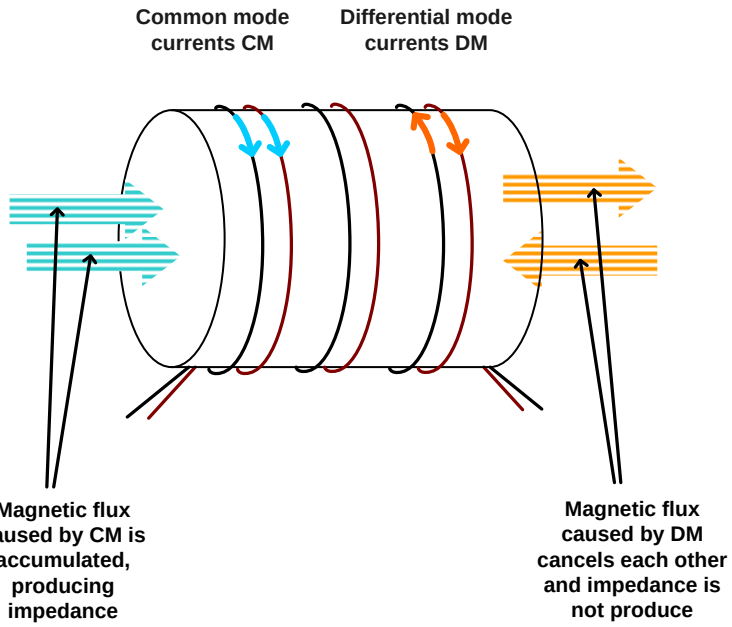

Figure 8: Magnetic flux in a common mode choke.

Fig. **9** presents a typical common mode choke under consideration: a choke with two symmetrical windings. The shape of the core is a toroidal. The study of the behavior of a common mode choke involves four types of impedances:

- *Common mode impedance*; it is the impedance faced by the common mode current in the choke.
- *Differential mode impedance*; it is the impedance faced by the differential mode current in the choke.

- *Inter-winding capacitance*; it is the parasitic impedance existing between two turns of a winding.
- *Intra winding capacitance*; it is the parasitic impedance existing between the two windings of the choke.

Table **1** lists the impedances of the common mode choke and their respective designable parameters. These designable parameters are the parameters that can be modified by the designer and will be the inputs of the behavioral model of the common mode choke.

Fig. **10** presents the general equivalent circuit of the common mode choke. The structure is validated *via* measurement in the next section. Z_{cm} is the common mode impedance, Z_{dm} is the differential mode impedance, C_{int} is the parasitic inter-winding capacitance and C_{tt} the parasitic intra-winding capacitance.

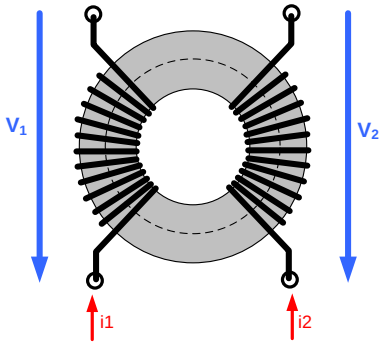

Figure 9: Typical CMC under consideration.

Table 1: Designable parameter for common mode choke

Impedances of the CMC	Designable parameters
Z_{cm}	*Material (complex permeability)* *Dimension of the choke* *Number of turns* *Effective length*
Z_{dm}	*Number of turns* *Dimensions of the choke* *Angle of the winding free section*
Inter and Intra Winding Capacitance	*Number of turns* *Dimensions of the choke* *Wire dimensions and materials(isolation and diameter)*

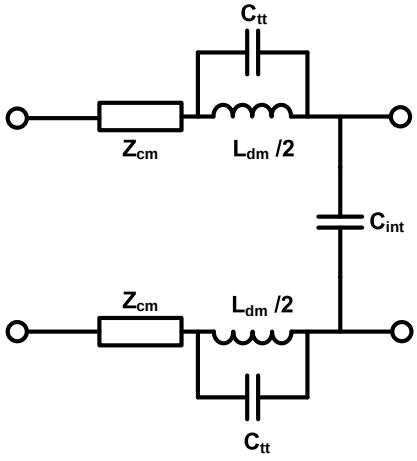

Figure 10: General equivalent circuit of the common mode choke.

Related Impedance Modeling

*Common mode impedance.*The value of the CM impedance is strongly related to the value of the permeability of the core. As detailed in [10] the inductor introduces frequency variable impedances in the circuit. Permeability of a common mode inductor is a complex parameter, the real component represents the reactive component and the imaginary part represents the losses. CM impedance of a CMC can be represented by the series equivalent circuit of a suppression core: the loss free inductor (L_s) is in series with the equivalent loss resistor (R_s). The following equation relates the series impedance and the complex permeability.

$$Z = R_s + j\omega L_s = j\omega L_o(\mu_s' - j\mu_s'') \quad \textit{where} \quad L_o = \mu_0 \frac{A_e}{l_e} N^2 \tag{1}$$

N: Number of Turns

A_e and l_e: Respectively the effective area and length of the choke under consideration.

The complex permeability of the material is assumed to be known from manufacturers' data sheets and/or simulation. A model of frequency dispersion of complex permeability in ferrites is proposed in [11]. The permeability spectra of ferrite materials can be described by the superposition of two kinds of resonance phenomena (domain-wall resonances and gyromagnetic spin rotation). They depend on the characteristic dispersion parameter and their values can widely differ from one material to another. Table **2** lists the values for two sintered materials. Fig. **11** represents the complex permeability of a sintered MnZn ferrite. The real and imaginary parts of the complex permeability can be modelled with the following equations:

$$\mu' = 1 + \frac{\omega_d^2 \chi_{do}(\omega_d^2 + \omega^2)}{(\omega_d^2 - \omega^2)^2 + \omega^2\beta^2} + \frac{\chi_{so}\omega_s^2[(\omega_s^2 + \omega^2) + \omega^2\alpha^2]}{[\omega_s^2 - \omega^2(1+\alpha^2)]^2 + 4\omega^2\omega_s^2\alpha^2} \tag{2}$$

$$\mu'' = \frac{\chi_{do}\omega\beta w_d^2}{(\omega_d^2 - \omega^2)^2 + \omega^2\beta^2} + \frac{\chi_{so}\omega_s\omega\alpha[\omega_s^2 + \omega^2(1+\alpha^2)]}{[\omega_s^2 - \omega^2(1+\alpha^2)]^2 + 4\omega^2\omega_s^2\alpha^2} \tag{3}$$

The terms (α, χ_{sc}) and (β, χ_{do}) are related to the spin component and the domain wall component respectively.

Figs. **11** and **12** present the simulated complex permeability of a sintered MnZn ferrite and the simulated CM impedance of a core made of this material respectively.

Table 2: Permeability Dispersion Parameters Of Sintered MnZn And NiZn Ferrite For Spin And Domain Wall Resonance

	Density (g/cc)	**Domain Wall Component**			**Spin component**		
		χ_{do}	**f_d (MHz)**	β	χ_{so}	**f_s (MHz)**	
MnZn Ferrite	4.9	3282	2.5	9.3*10e+6	1438	6.3	1.28
NiZn Ferrite	5.2	485	2.8	3.5*10e+6	1130	1100	161

Differential mode impedance. The value of the DM impedance is related to leakage inductances. Fluxes created by the differential mode currents do not completely cancel each other: parts of these currents leak from the choke in between the wiring system. For a more accurate estimation, formulae are available in the literature [12].

Parasitic capacitances. Parasitic stray capacitance is composed of the winding capacitance (C_w, C_w') and the turn to turn capacitances (C_{tt}, C_{tt}'). The winding capacitances tend to decrease the efficiency of the CMC while the turn to turn capacitances tends to improve the differential mode current attenuation. Intra winding capacitances are negligibly small in most applications. Detailed formulae to model these impedances are available in [7] and [8].

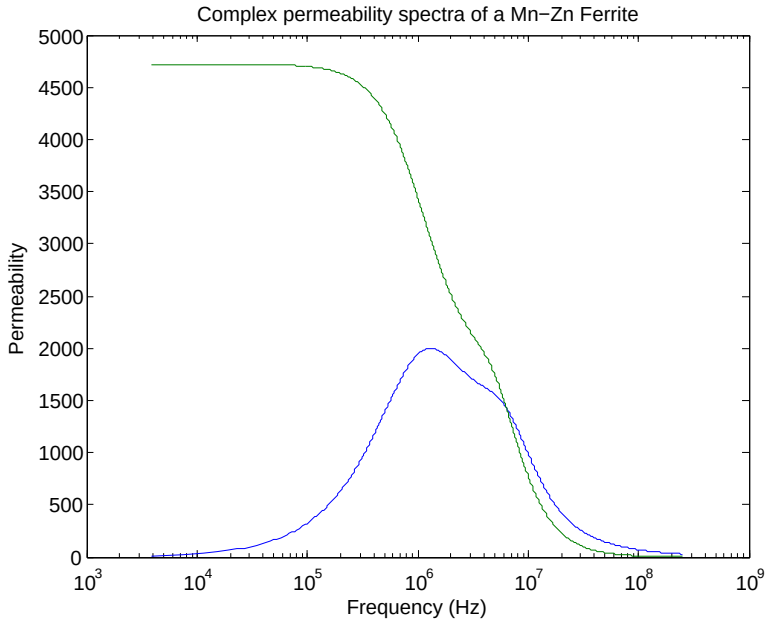

Figure 11: Complex permeability spectrum of a Sintered MnZn ferrite.

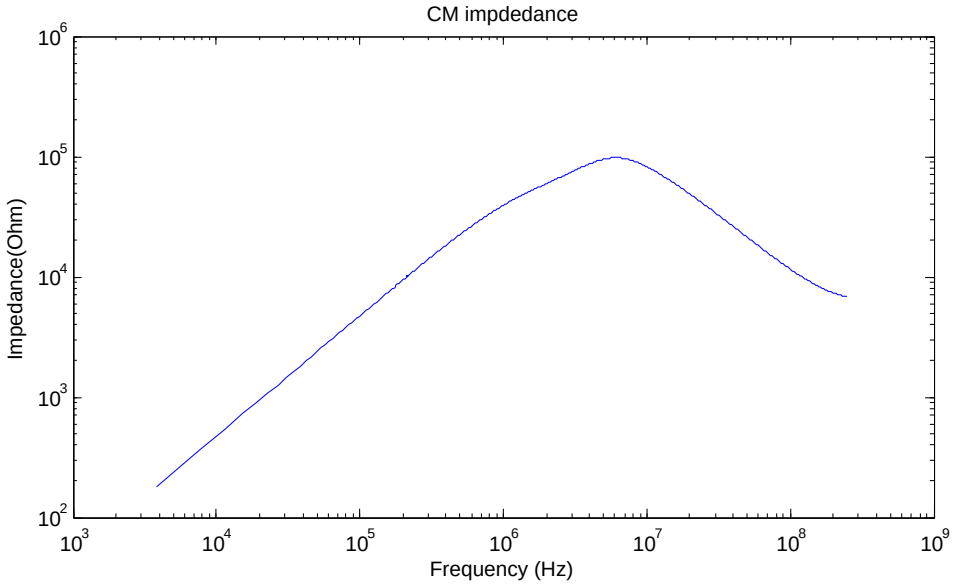

Figure 12: Simulated complex CM impedance of a MnZn core (Dimension: 25*10*5 mm, N=20).

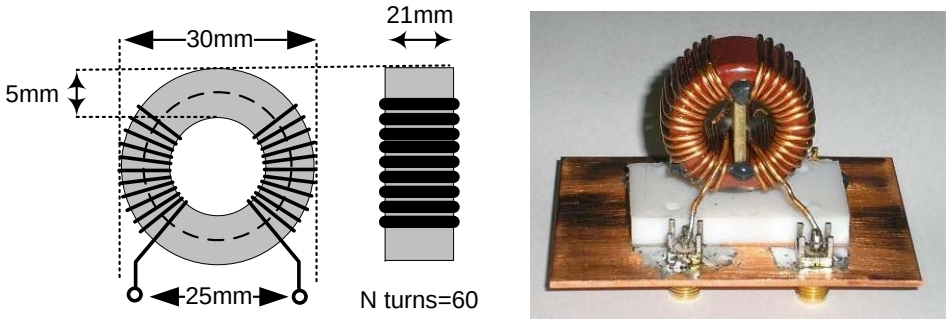

(a) Dimensions (b) Set-up

Figure 13: CMC under test.

Measurements

Measurements setup. Measurements have been performed on a common mode choke presented in Fig. **13**. Four SMA (SubMiniature version A) connectors are connected to the four ports of the choke through a copper plate. It is then ensured that the ground of the measurement device is a reference plane which conducts the return currents. The core used as the main example in this chapter is a ferrite made of MnZn. Its characteristics have been measured with an Impedance/Gain-Phase Analyzer (HP 4194A) between 100 Hz and 40 MHz. Results are presented in Fig. **15** and **16**. This auto balancing bridge method [9] offers wide frequency coverage and is specially adapted to the ground device measurements. The test set-up used to measure the four characteristic impedances of the choke is detailed thereafter.

Measurements of coil inductance. Coil inductance can be measured directly by connecting the instrument as shown in Fig. **14-a**. All other windings should be left open. The inductance measurement includes the effects of capacitances. If an equivalent circuit analysis function is available, individual values for inductance, resistance and capacitance can be obtained. This measurement is used to extract the value of the turn to turn capacitances.

Measurements of the leakage inductance. It can be measured by connecting the output port of the first windings to the input port of the second winding to reproduce the circuit as seen by the differential mode current. The measurement is described in Fig. **14-b**.

Inter winding capacitance measurement. It is the capacitance between the two coils. It is measured by connecting one side of each winding to the instrument as shown in Fig. **14-c**. The other sides are left open.

Measurement of the common mode impedance. The inputs and the outputs windings are connected together and reproduce the circuit as seen by the common mode current, as shown in Fig. **14-d**.

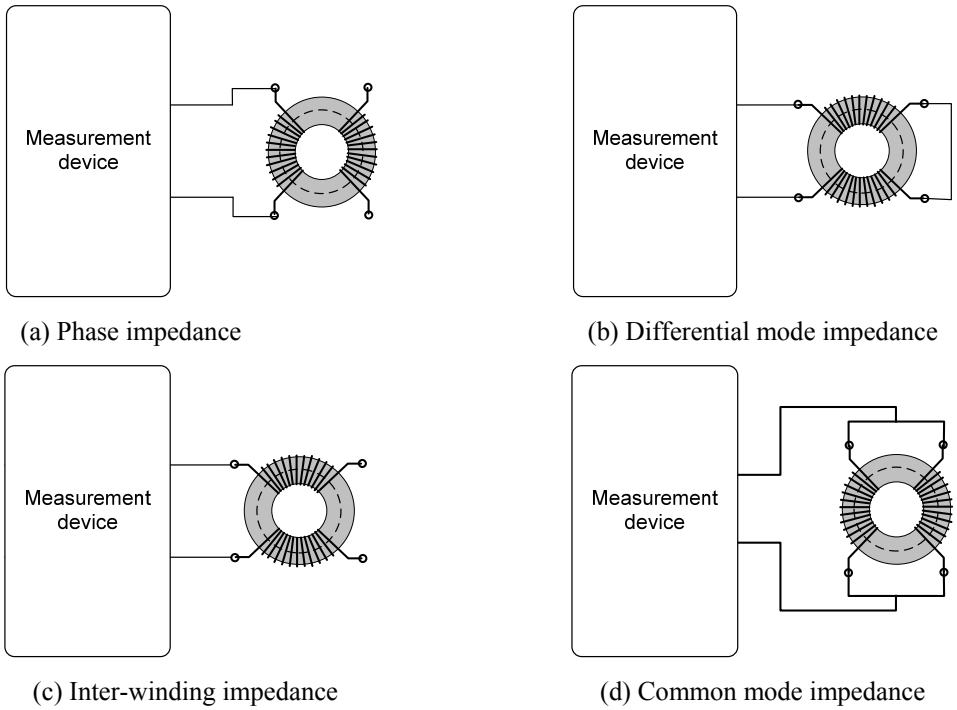

(a) Phase impedance (b) Differential mode impedance

(c) Inter-winding impedance (d) Common mode impedance

Figure 14: Impedances measurement.

Measurements results. The choke under consideration is bonded with a copper wire with a diameter of 0.99 mm. Its insulation in polyurethane has a thickness of 12 µm. The choke can be used with a rated current of 5A and nominal voltage of 250 Vac. The measured impedances are presented in Figs. **15** and **16**.

The equivalent circuit of the measured impedance of the common mode choke can be extracted from the measurement results shown in Figs. **15** and **16**. The equivalent circuits of the measured impedances are shown in Fig. **18**:

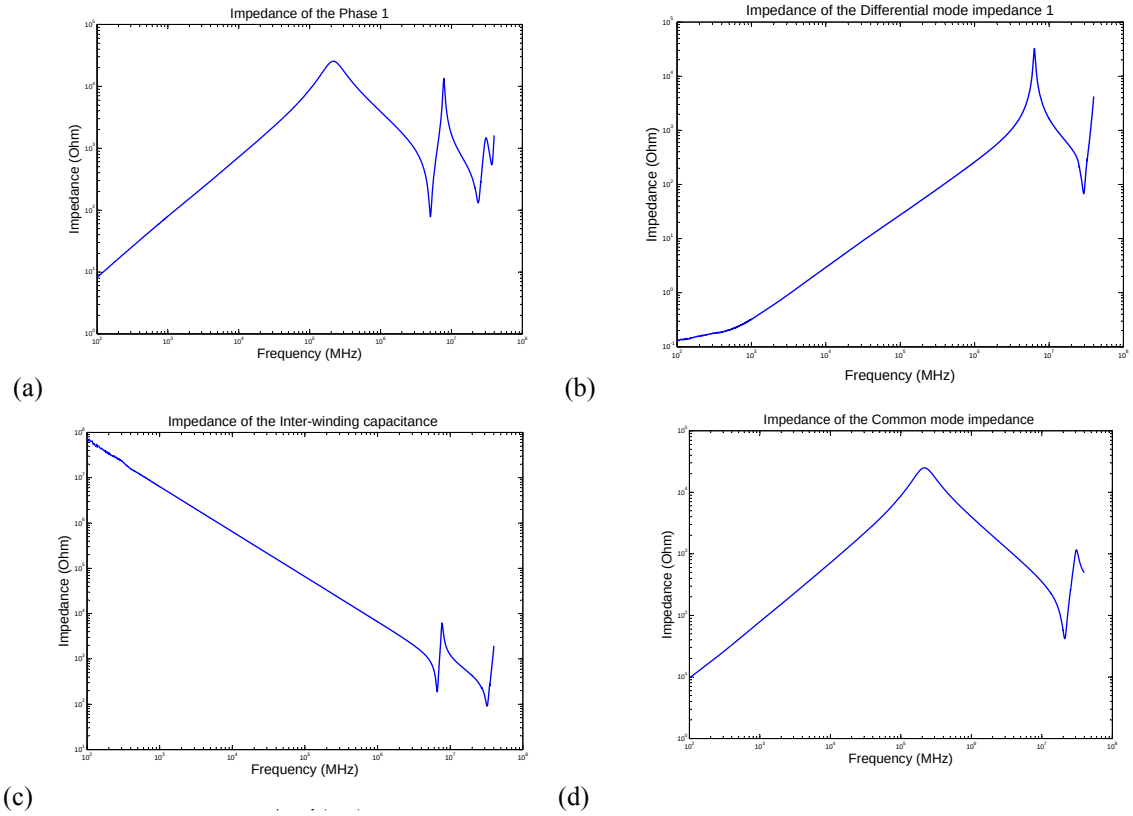

Figure 15: Measured impedances of the common mode choke under test.

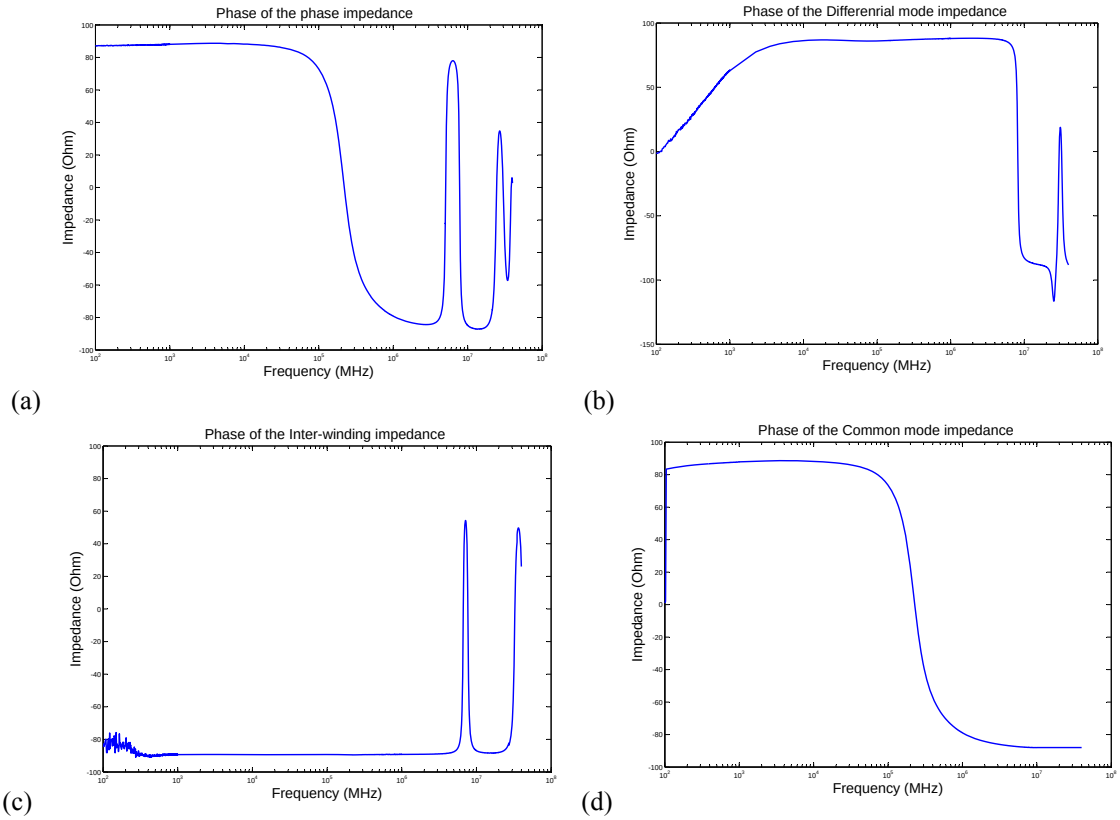

Figure 16: Measured phases of the common mode choke under test.

- The measurement of the leakage inductance (Fig. **15-b**) is independent of the inter-winding capacitances which is short circuited. The common mode fluxes generated by the windings cancel each other in this configuration. The leakage inductance resonate with the parallel turn to turn capacitance on each side of the choke This resonance can be used to extract the total value of the turn to turn capacitance which consists of two capacitances in series in this measurement configuration. The value of each turn to turn capacitance is double of the extracted value.
- The resonance between the turn to turn capacitance and the leakage inductance is also visible in the respective phase impedance in the Fig. **15-a**. It suggests that the common mode impedance is in series with half the differential mode impedance. The phase impedance remains indeed identical to the common mode impedance before this resonance. It shows that the common mode impedance is not in parallel with the turn to turn capacitance which is then only parallel with half the leakage inductance. An explanation of this structure is that the leakage flux within the wiring system interacts only with the turn to turn capacitance while the main fluxes remaining inside the choke do not.
- The anti-resonance visible in the inter-winding capacitance is related to its position in series (Fig. **15-c**) with the parallel structure formed by the differential mode impedance and the turn to turn capacitances in series with the common mode impedance.
- The measured common mode impedance is presented in Fig. **15-d** and is independent of the leakage inductance. The leakage fluxes have cancelled each other.

Fig. **17** compares the measured impedances of the choke with the modelled one. The extracted values from the measurements have been used and the good agreement between the two confirms the structure of each equivalent circuit. These results allow a clear identification of the components related to the differential mode (leakage inductance, inter-winding capacitance and turn to turn capacitances) and the common mode (common mode impedance only).

The common mode current flowing in the choke faces twice the common mode impedance in each winding as the flux on created on both sides add to each other in each winding. Both the phases are in parallel with each other as far as the common mode current is concerned. The final equivalent circuit, presented in Fig. **18**, is then equivalent to single common mode impedance. Fig. **19** shows equivalent circuits of the measured impedance.

BEHAVIORAL MODEL FOR COMMON MODE CHOKES

Criteria of a Behavioural Model of Common Mode Choke

Major criteria for behavioural modelling of common mode chokes are:

- The noise spectrum of EMI in frequency convertors is usually spread from around 10 kHz to several decades of MHz. The frequency dependence of parameters of the choke has to be taken into account to provide an accurate model even at higher frequencies.
- The model is predictive: it is assumed that designers do not have access to a prototype and experimental values. The usage of models as “scaled circuit” is not possible in this configuration. In addition to electrical information like voltages and currents, others parameters of the predictive model have to be provided by literature or manufacturers.
- The prediction method has to permit the integration of all parasitic elements. In software widely used like Pspice ®, it leads to very small time constants and to serious convergence problems.
- A common problem of common mode chokes is the magnetic saturation. Specific attention in its modelling is required.
- Time domain as well as frequency domain is needed by designers.
- The predictive model will be a ‘black box’ for designers. It only requires several parameters as inputs and provides outputs needed in graphs or tables.

The software Simulink ®, for its user friendly interface and its combined usage with Matlab ®, is chosen to develop the model presented.

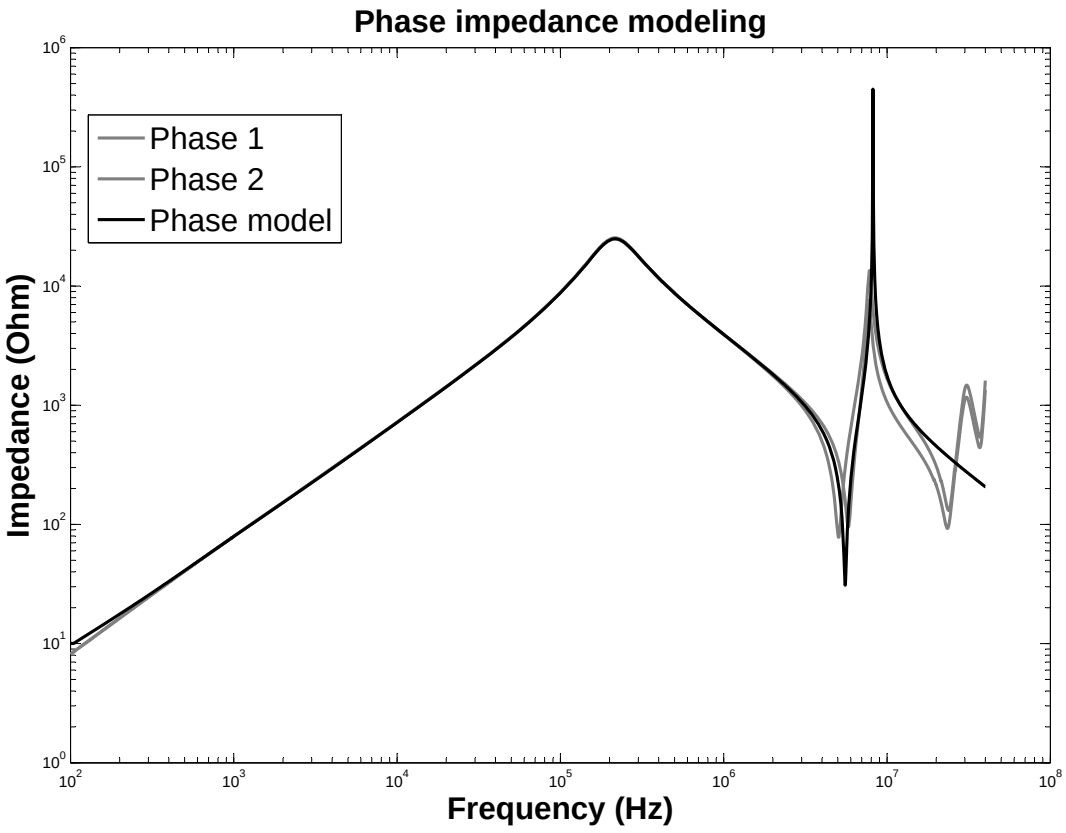
Phase impedance modeling
Phase 1
Phase 2
Phase model
Impedance (Ohm)
Frequency (Hz)

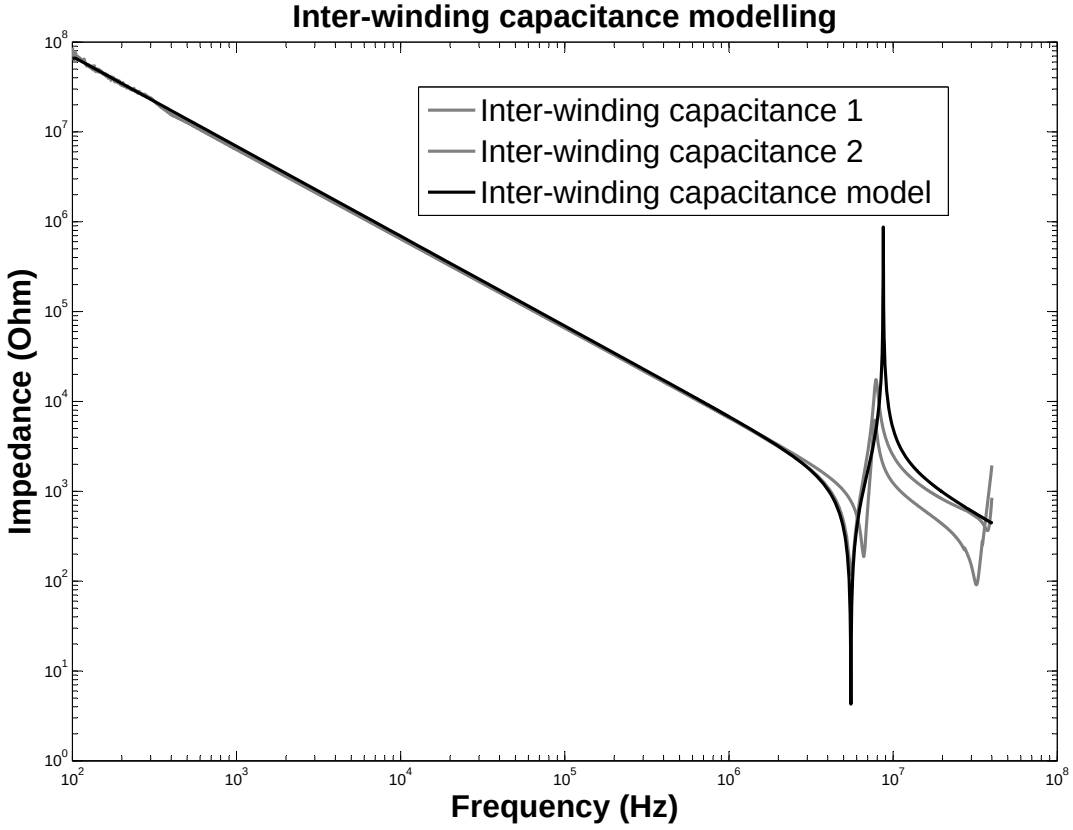
Inter-winding capacitance modelling
Inter-winding capacitance 1
Inter-winding capacitance 2
Inter-winding capacitance model
Impedance (Ohm)
Frequency (Hz)

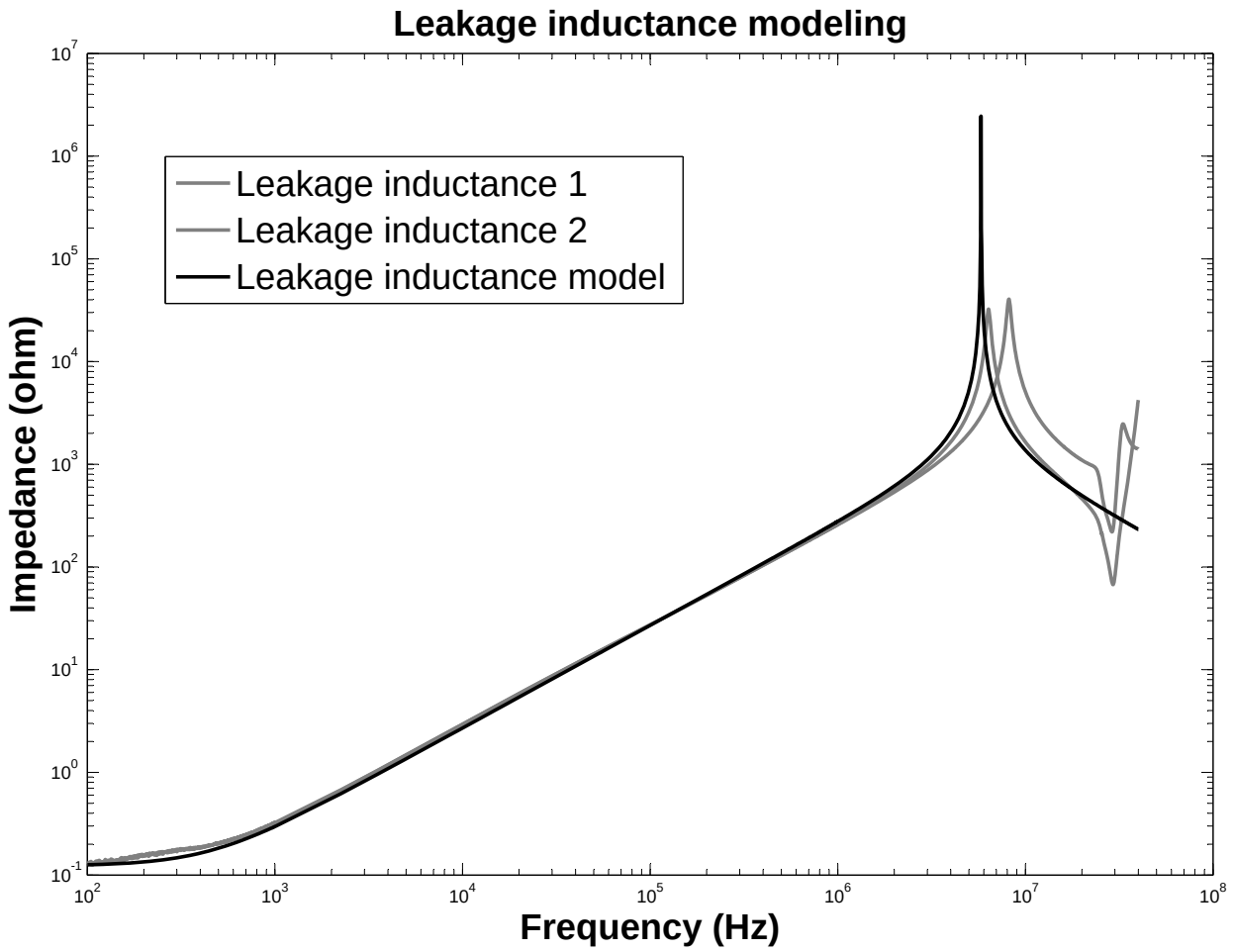

Figure 17: Comparison of the measured impedances of the choke with the modeled impedances (Extracted values).

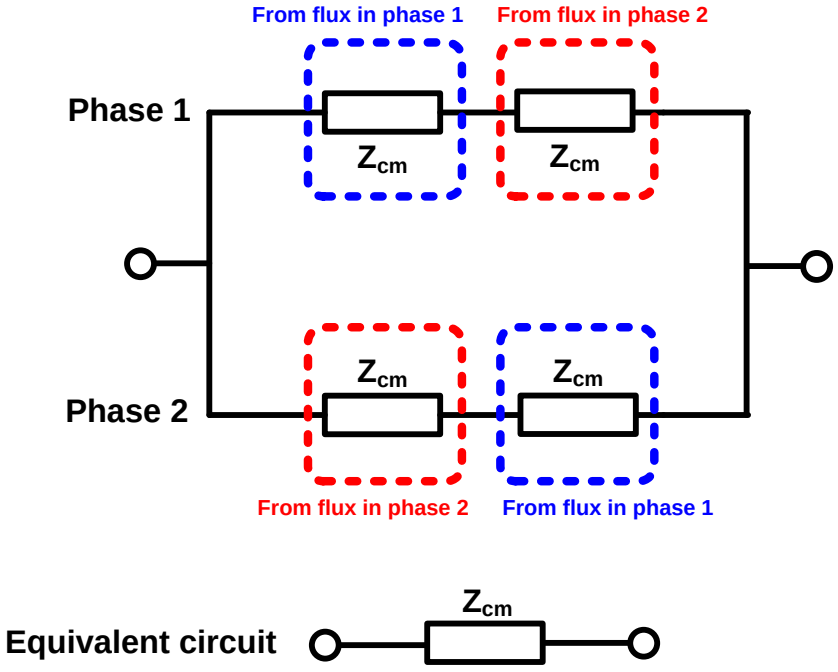

Figure 18: Equivalent common mode circuit of the choke.

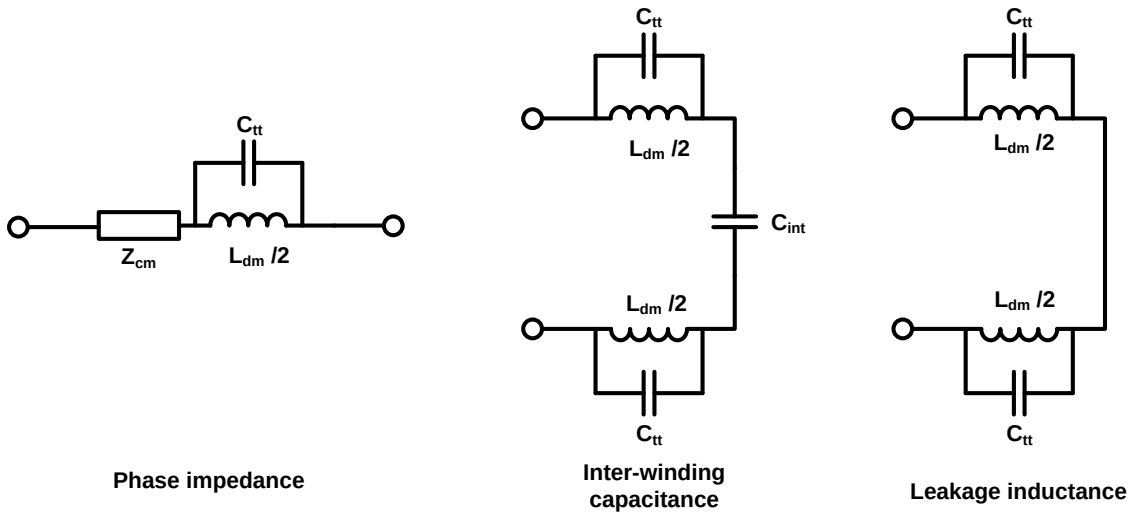

Figure 19: Equivalent circuits of the measured impedances.

Topology of the Model

An overview of the topology of the model in consideration is presented in Figure 20. The topology of the model is based on a translation of the common choke in its electrical equivalent circuit 'in situ' for the common mode and the differential mode. The electrical equivalent circuit includes the following impedances: common mode and differential mode impedances and parasitic capacitances (turn to turn and intra-windings). It is assumed that the common mode filter is placed as close as possible to the output of the converter.

In this condition the characterisation of the environment of the choke, performed 'in situ', should include only 2 impedances for a grounded system with 2 phases: the input asymmetrical impedance of the cable and its load, and the phase to phase impedance of this same system. The converter is assumed to be voltage regulated. The attenuation of the common mode and the differential mode currents in the cable is then only dependant on the filter and the converter environment. This 'in situ characterisation' of the performances of the common mode choke allows all the parasitic upstream of the motor drive to be included.

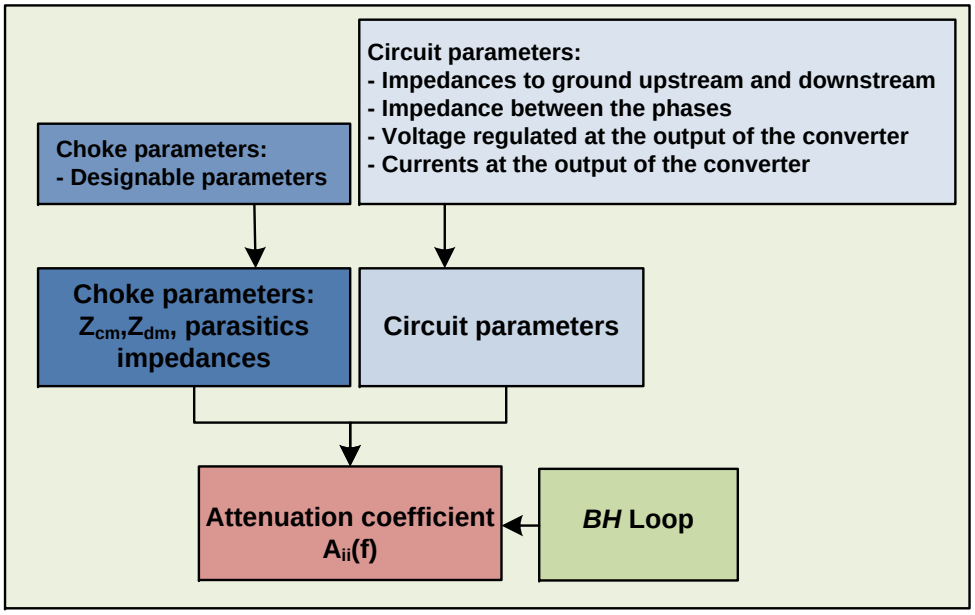

Figure 20: Topology of the behavioral model for CMC.

The designer has to find the measured or simulated currents value where the CMC will be placed later. The modification factors are first calculated in the frequency domain. If the output currents are measured in a time domain, it is important to sample the measurements properly in order to include all the high frequency characteristics of the noise.

Modification Factors Calculations

Electrical equivalent networks. Two electrical circuits are considered to characterize the attenuation of the common mode current and the differential mode current. The Fig. **21** and the Fig. **22** present the differential mode and the common mode equivalent circuit of the output of the converter with and without the choke respectively. In these circuits, Z_a refers to the asymmetrical input impedance of the cable and its motor, Z_m is the phase to phase input impedance of the motor and its cable.

These two impedances include for Z_a eventual Y-capacitors added in the common mode filter, and in the case of Z_m eventual inductors and X-capacitors added in a differential mode filter. These two impedances are also fully characterizing the circuit upstream of the converter and take into account all parasitic. The differential mode impedance Z_{dm} is formed by the leakage inductance (Z_{Ldm}) parallel to the turn to turn capacitance (Z_{CTT}) as described in the previous section and is expressed as:

$$Z_{DM} = \frac{Z_{LDM}.Z_{Ctt}}{Z_{Ctt} + Z_{LDM}} \quad \textbf{(4)}$$

In the same setup, the inter-winding capacitance (Z_{cint}) of the choke is associated with the impedance Z_m. The new impedance Z_3 is then expressed as:

$$Z_3 = \frac{Z_m.Z_{C\text{int}}}{\left(Z_m + Z_{C\text{int}}\right)} \quad \textbf{(5)}$$

Currents I_{DM1} and I_{CM1} are the CM and DM currents initially flowing at the output of the frequency converter. Currents I_{DM2} and I_{CM2} are the CM and DM currents at the output of the frequency converter when the common mode choke is placed in the circuit. The attenuation of common mode current and differential mode currents is of interest in this study.

Expression of the Modification Factor for the Differential Mode Current

In the setup described in Figure 21, the differential mode currents I_{DM1} and I_{DM2} can be expressed as followed:

$$\begin{cases} V_{dm} = I_{DM1}.Z_m \\ V_{dm} = I_{DM2}.(Z_3 + Z_{dm}) \end{cases} \quad \textbf{(6)}$$

The differential mode current modification factor Att_{dm} is:

$$\begin{cases} I_{DM2} = Att_{dm}.I_{DM1)} \\ Att_{dm} = \dfrac{Z_m}{(Z_3 + Z_{dm})} \end{cases} \quad \textbf{(7)}$$

Expression of the Modification Factor for the Common Mode Current

In the setup described in Fig. **22**, the common mode currents I_{CM1} and I_{CM2} can be expressed as followed:

$$\begin{cases} V_{cm} = I_{CM1}.Z_a \\ V_{cm} = I_{CM2}.(Z_a + Z_{cm}) \end{cases} \quad \textbf{(8)}$$

The common mode current modification factor Att_{cm} is:

$$\begin{cases} I_{CM2} = Att_{cm}.I_{CM1} \\ Att_{cm} = \dfrac{Z_a}{(Z_a + Z_{cm})} \end{cases} \quad \textbf{(9)}$$

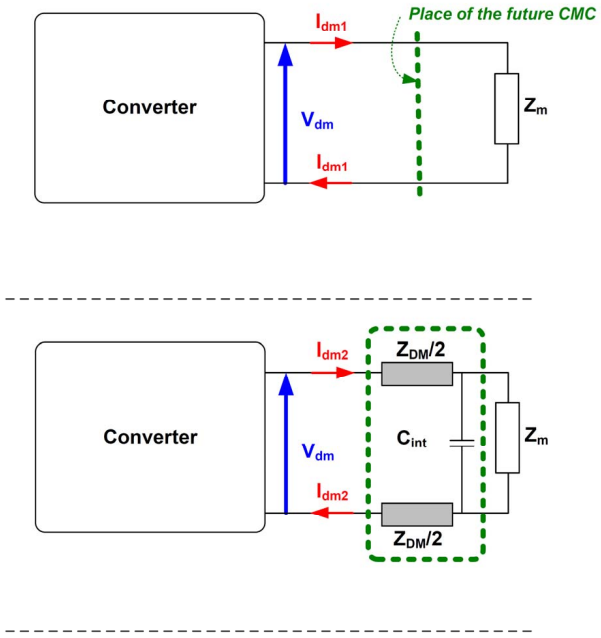

Figure 21: Differential mode equivalent circuit with and without the choke.

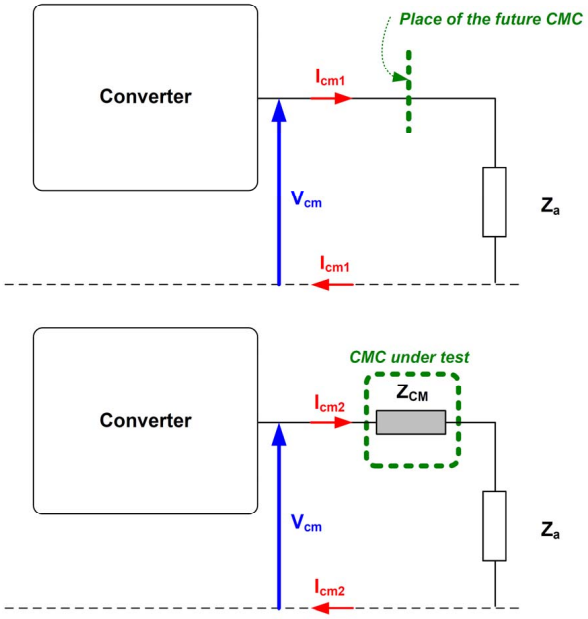

Figure 22: Common mode equivalent circuit before and after insertion of the choke.

Discussion on the Stability of the Noise Voltage

The converter has a regulated output voltage (this model can be adapted to a converter with current control). Stabilized-voltage power supplies have extremely low output impedance, often less than 1mΩ. The different techniques used in voltage control are presented in [27] and [26]. It is assumed that the common mode output noises voltage V_{cm} remains identical when the choke is connected to the circuit. In case the common mode noise voltage and/or the differential mode voltage change, these changes can be inserted in the model. Its /their variations between the two setups are then evaluated by the designer and can be introduced as:

$$Att_{dm} = \frac{Z_m}{(Z_3 + Z_{dm})}.(1 + \Delta V_{dm}) \quad \textbf{(10)}$$

$$Att_{cm} = \frac{Z_a}{(Z_a + Z_{cm})}.(1 + \Delta V_{cm}) \quad \textbf{(11)}$$

and ΔV_{cm} are the variation of common mode and differential noise voltages with of the choke respectively. These variations well are as complex numbers as the impedances and depend on the frequency. The deviation calculation introduced in the next section can also be used to study the stability of the modification factors in case these variations exist and cannot be evaluated.

Modification Factors Evaluation

Fig. **23** shows the overall model used to calculate of the modification factors. All impedances considered are complex numbers: arguments as well as phases have been included.

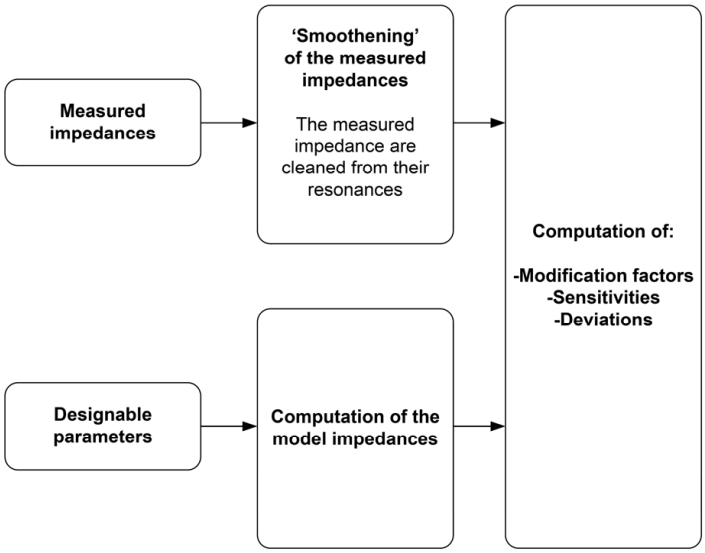

Figure 23: Overview of the model to calculate the modification factors.

Differential mode modification factor. Fig. **24** presents the choke impedances used for the differential mode current modification factor computation: the leakage inductance, the turn to turn capacitance and the input impedance between the two phases of the motor and its feeder. Four values for the capacitances have been considered between 500 pF and 2 nF. The relevance of these values is further developed in the last section of this chapter.

Two common mode chokes are considered as examples and named 'common mode chokes 1 and 2'. They are both MnZn ferrites as used in the measurements of section 0 of this chapter. The choke number 1 and 2 have 14 and 30 turns, respectively.

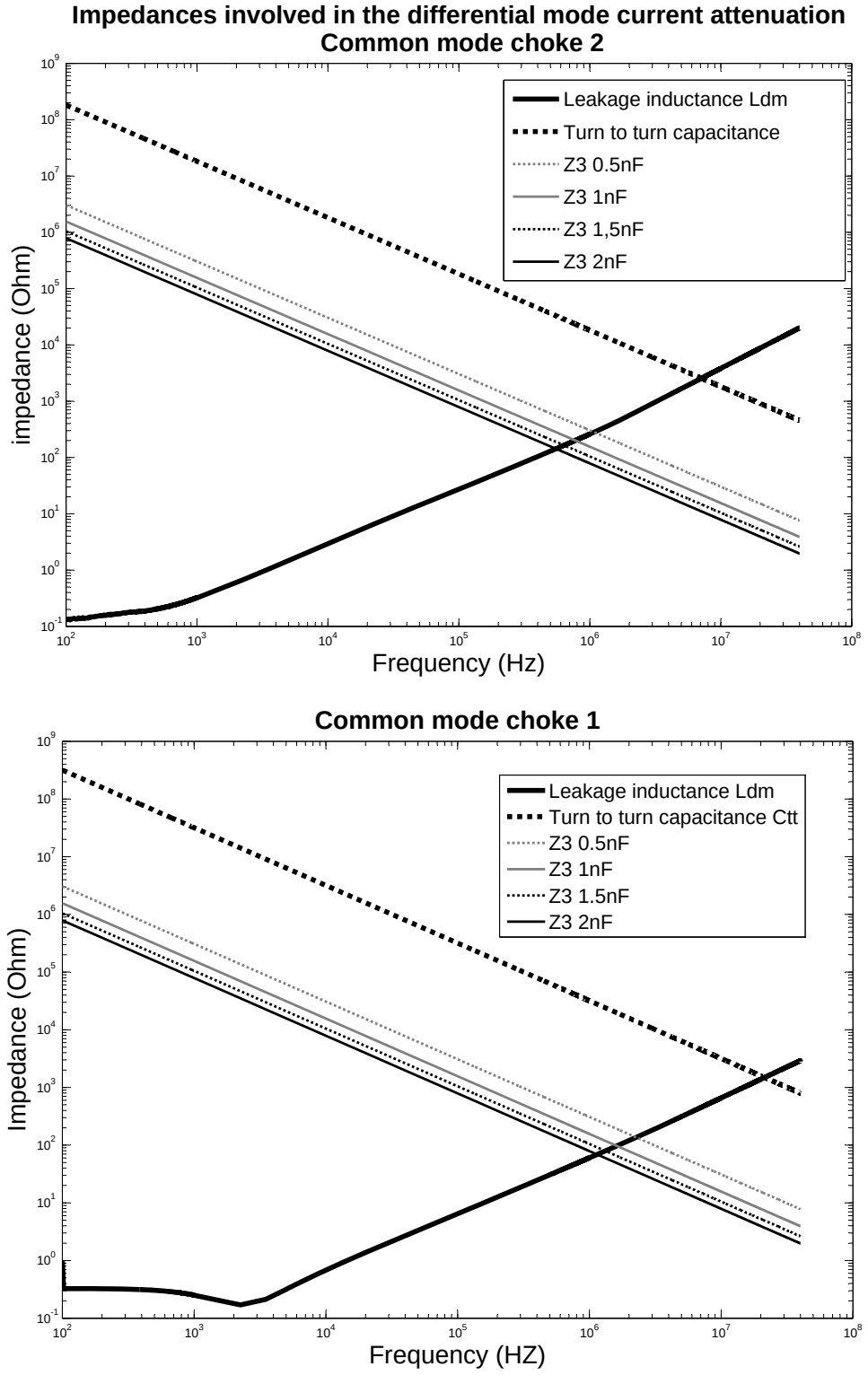

Figure 24: Differential mode impedances and variable capacitances between the phases of chokes vs. Frequency.

The Fig. **25** presents the expected differential mode modification factors with variable input cable impedances. These factors are mainly driven by the resonances of the leakages inductance with Z_m and Z_{ctt}. The resonant frequencies can be graphically evaluated at the intersection of the norm of the concerned impedances in Fig. **25**. As

the frequency increases, the first resonance happens between the leakage inductance and the cable input impedance and marks the beginning of the attenuation as well as a substantial increase of the differential mode current. For the common mode choke 1 and 2 these resonances occur around 1 MHz. This increase can be a design issue for the engineers. The study of the sensitivity and the deviation of the design can be used to optimize the choke accordingly.

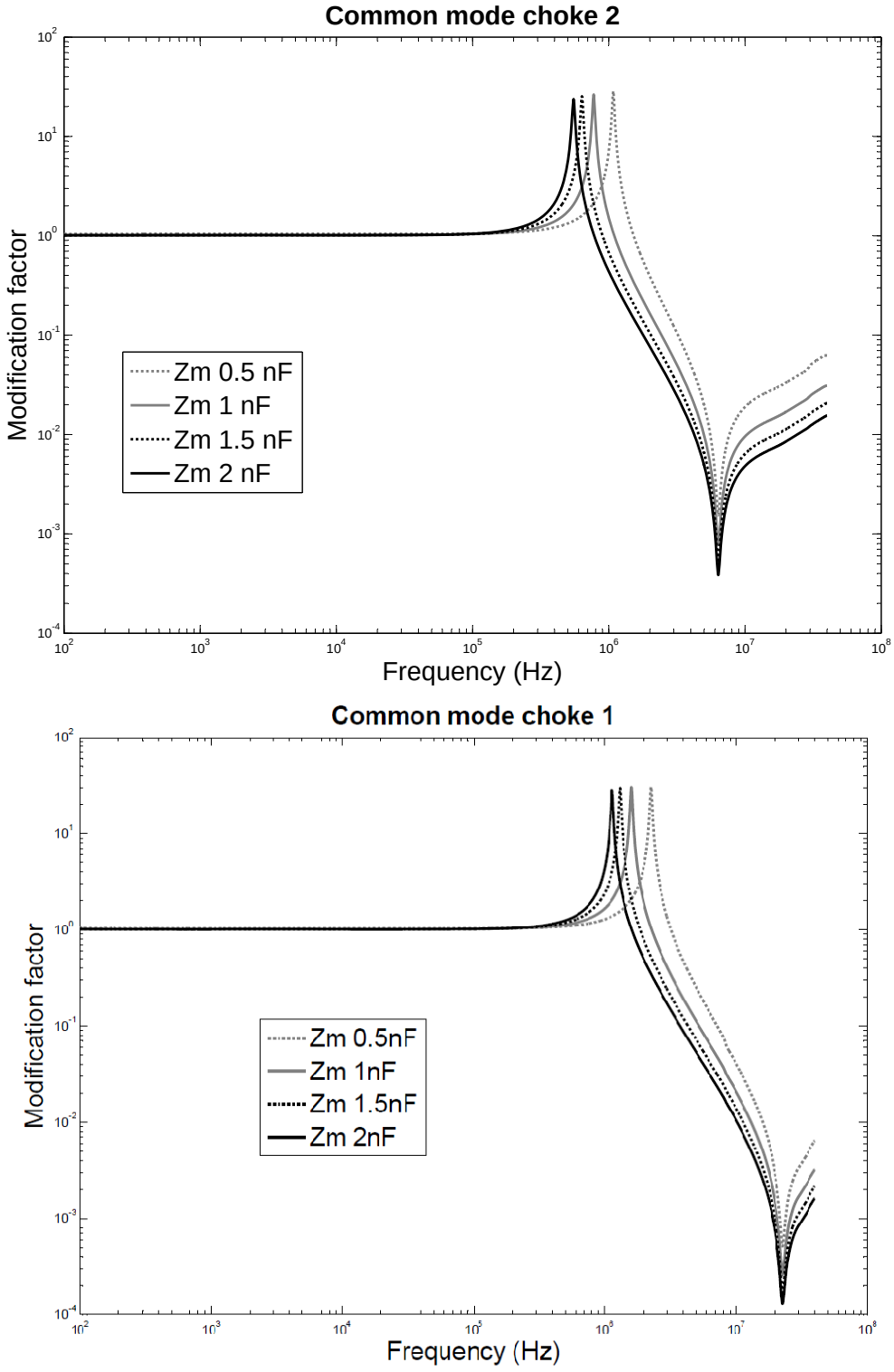

Figure 25: Differential mode modification factors with variable input cable impedance.

The maximum attenuation is reached at the resonances between the turn to turn capacitances with the leakage inductance. In the two examples the current is attenuated in the order of a thousand at the maximum attenuation. In general the attenuation of the differential mode current occurs in a narrower frequency band than the common mode one. While it is not the main purpose of the common mode choke, its prediction is however useful to forecast and prevent an eventual increase of differential mode noise in the overall filter design and/or optimize the attenuation of differential mode noise in conjunction with differential mode inductors and X-capacitors.

Common mode modification factor. Fig. **26** presents the impedances of the chokes used for the common mode current modification computation: the common mode impedance and the impedance to ground where the choke is placed. The same two common mode chokes 1 and 2 are considered.

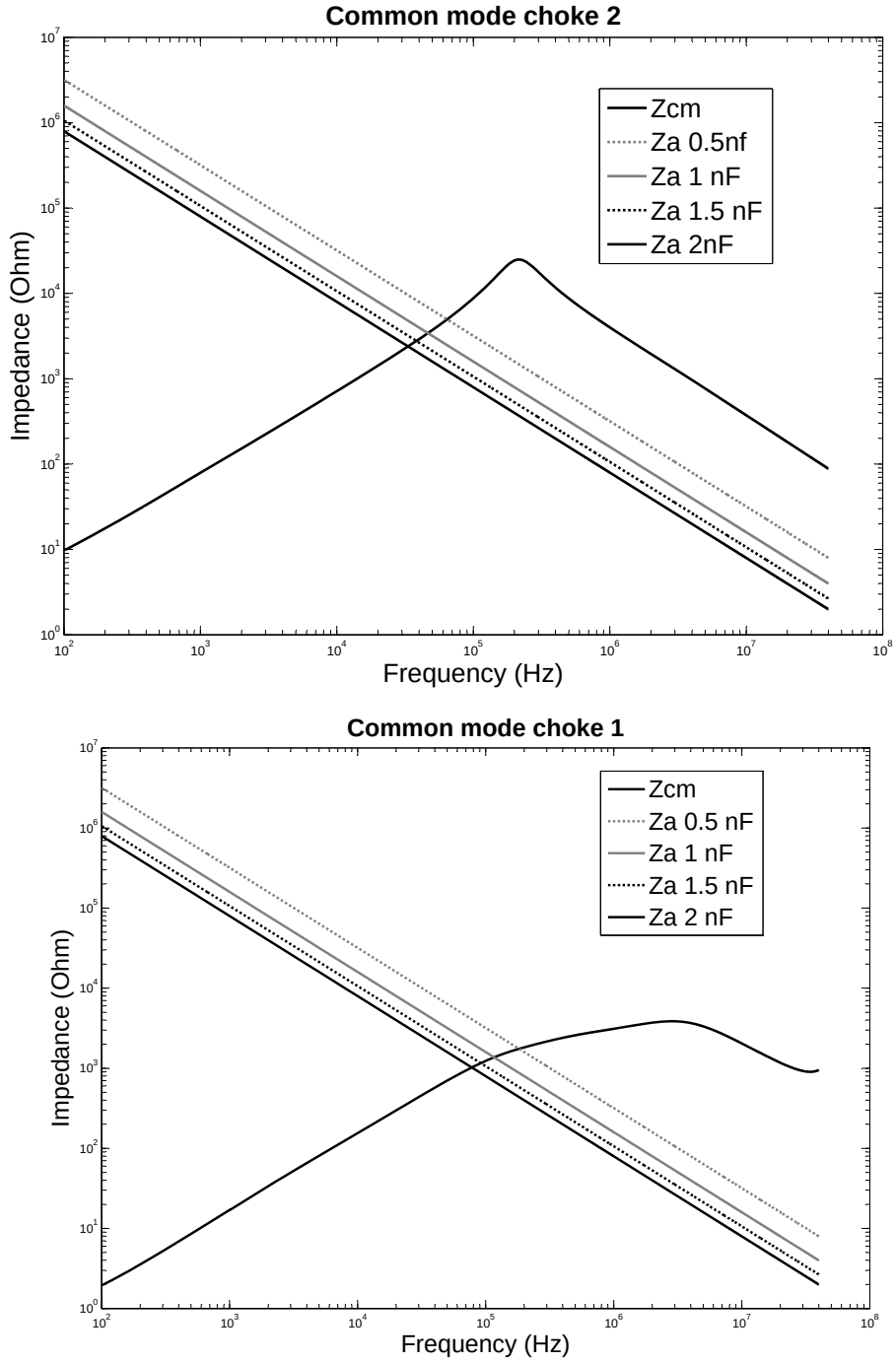

Figure 26: Common mode impedances and variable capacitances to ground of chokes vs. Frequency.

Fig. **27** presents the expected common mode modifications with variable impedance to ground. Four values of capacitance have been considered between 500 pF and 2 nF. The relevance of these choices is further developed in the last section of this chapter.

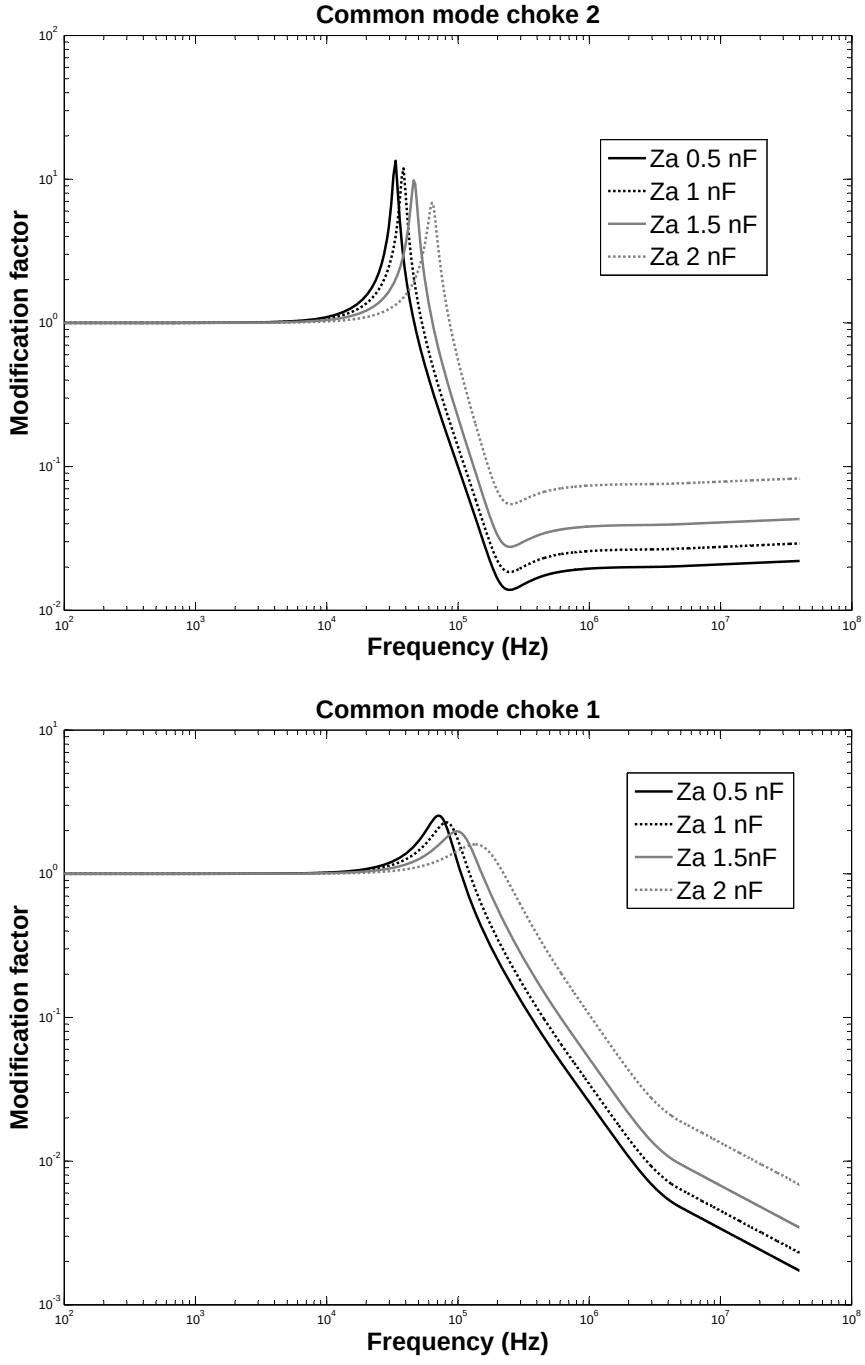

Figure 27: Common mode modification factors with variable capacitances to ground.

These modifications are mainly driven by the resonances of the impedances to ground with the common mode impedance. The resonant frequency can be graphically evaluated at the intersection of the norm of the concerned impedances shown in Fig. **26**. Likewise for increasing frequencies, the first resonance happens between the common mode impedance and the impedance to ground; and marks the beginning of the modification with a substantial increase of common mode current which can be a design issue. The study of the sensitivity and the deviation of the

design can be used to design the choke accordingly. The importance of the increase of the common mode current is strongly related to the shape of the common mode impedance: a higher derivative coefficient of the impedance at the intersection point will result in a higher increase of the common mode current.

The maximum attenuation is not necessarily reached at the maximum common mode impedance value. The shape of the modification at high frequencies is related to the difference of impedance between the common mode impedance and the impedance to ground. For the common mode choke 1, this difference in impedance and the attenuation remains constant when the maximum attenuation is reached at the maximum value of the common mode impedance. For the common mode choke 2 however the difference between the common mode impedance and the impedance to ground increases after the initial resonance and the modification factor increases as well.

Saturation Modelling

To predict the performance of the common mode chokes accurately, a saturation model applicable under both steady state and transient magnetic excitations would be necessary. It is however possible in the first approximation to consider that the initial permeability remains same, as described in section 3 of this chapter. The saturation level is usually provided by manufacturer. This depends on the material, the size of the core and the number of turns.

MEASUREMENTS

Impedances Measurements

Two common mode impedances are measured:

(a) The input common mode impedance of the load and its cable where the choke is inserted

(b) The same impedance with the choke under test.

The common mode modification factor is obtained by dividing the input common mode impedance (a) by the one including the choke under test (b).

The Fig. **28** shows the measured input common mode impedance of the load and its cable between 20 kHz and 40 MHz frequency range. This impedance can be approximated by a capacitance of 20pF.

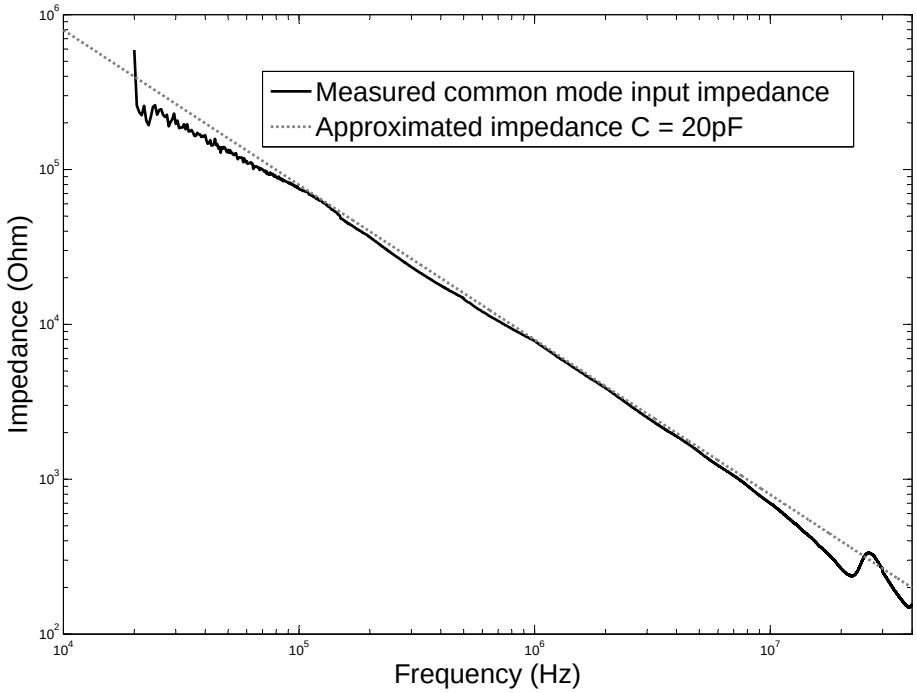

Figure 28: Input common mode impedance of the load and its cable.

The validation of the model of the common mode current modification factor is shown in Fig. **29**; the modeled attenuations are compared with the measured attenuations. The modeled attenuations are also calculated using the measured impedances of the choke 1 and 2 and approximated impedance to ground of 20pF which is shown in Fig. **28**. There is a very good agreement between the modeled and the measured values. The differences between the two curves associated with the chokes are due to the approximation of the impedance to ground with a capacitance. It is always better for the designer to use the actual impedance to ground in the simulation.

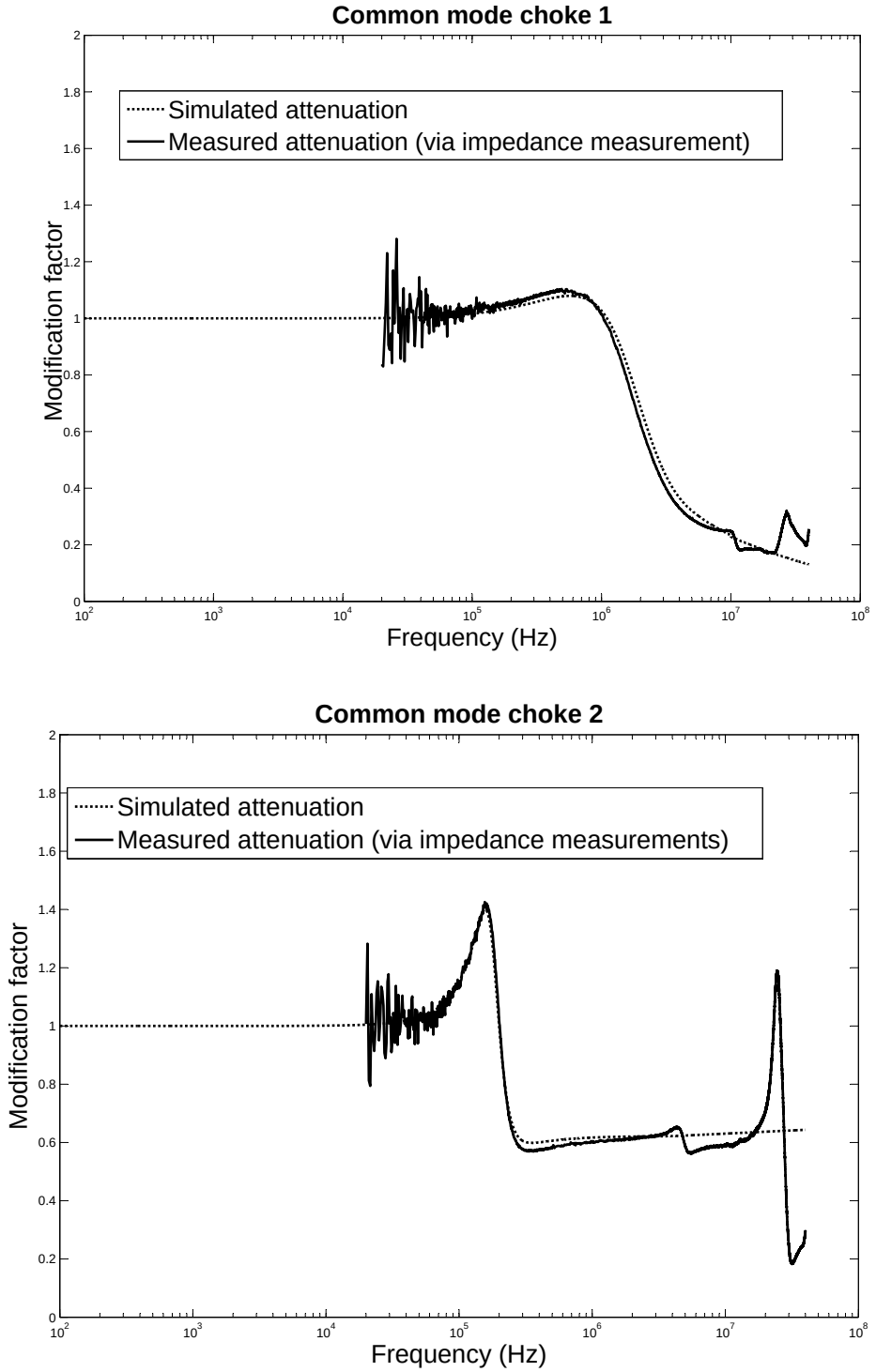

Figure 29: Modification factors: validation of the model *via* impedance measurements.

Current Modification Factor Measurements

Two common mode currents are measured:

(a) The input common mode current of the load and its cable where the choke is inserted,

(b) The same current when the choke under test is inserted.

The common mode modification factor is obtained by dividing the input common mode current (a) by the one including the choke under test (b).

The validation of the model of common mode current modification factor is shown in Fig. **30**: the modeled attenuations are compared with the measured attenuations. There is a very good agreement between the modeled and the measured values.

SENSITIVITY AND DESIGNABLE PARAMETERS

Sensitivity

Sensitivity studies provide additional insight into the behavior of the choke by understanding of how variations of parameters (for instance values of elements) influence the final performance [18], [19]. These studies are needed to take into account design variations.

The sensitivity studies can be performed at two levels. The local approach is based on a first order approximation which is mainly used to evaluate the effect of the error related to modelling or measurements of impedance and is not suitable for large variations. The normalized simplest sensitivity is the derivative function F with respect to any parameter h:

$$S_h^f = \frac{\partial \ln F}{\partial \ln h} = \frac{h}{F}\frac{\partial F}{\partial h} \qquad \textbf{(12)}$$

When a large change occurs in the system, large change sensitivity can be considered. This study is especially relevant when an engineer wants to change the designable parameters (material, size of choke or number of turns).

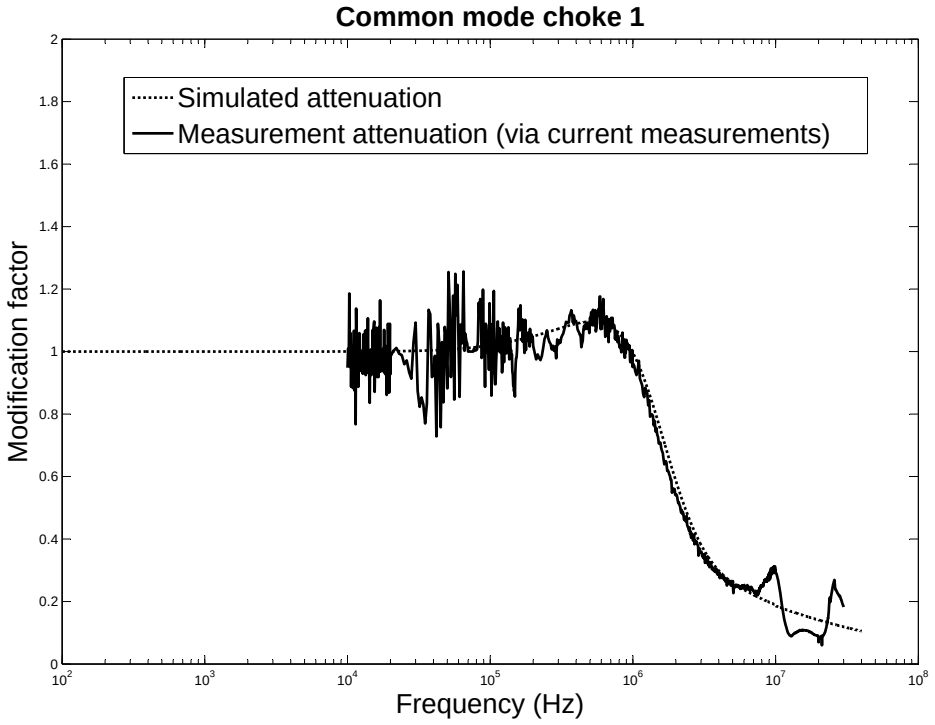

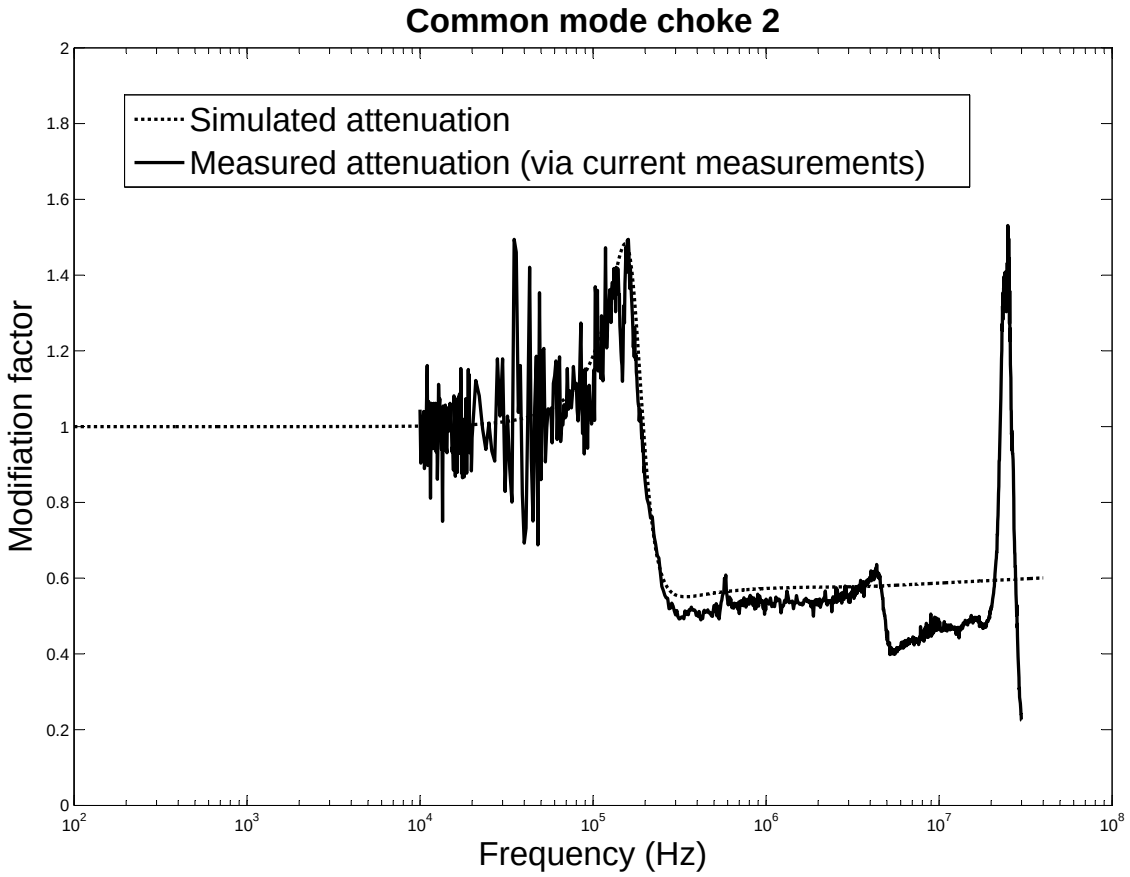

Figure 30: Modification factors: validation of the model *via* impedance measurements.

The large change sensitivity is based on a modification of the original system (the modification factors) by a low rank matrix [19].

Local sensitivity and the common mode modification factor. The common mode current modification factor is related to the common mode impedance and the impedance to the ground. The local sensitivity of the common mode impedance S_Z_{cm} and the local sensitivity of the impedance to ground S_Z_a are expressed as:

$$\begin{cases} S\_Z_{CM} = \dfrac{Z_a}{Att_{cm}} * \dfrac{\partial Att_{cm}}{\partial Z_a} = \dfrac{Z_{CM}}{(Z_a + Z_{CM})} \\ S\_Z_a = \dfrac{Z_{cm}}{Att_{cm}} * \dfrac{\partial Att_{cm}}{\partial Z_a} = -\dfrac{Z_{CM}}{(Z_a + Z_{CM})} \end{cases} \quad \textbf{(13)}$$

Fig. **31** presents the curves of local sensitivity of the common mode impedance and the impedance to ground for the common choke 1 and 2 presented in the previous section of this chapter. The local sensitivity has been initially expressed with the software Maple. The derived functions have then been embedded in a Simulink model. The modification factors and the choke parameters are then used as inputs in the model.

The common mode impedance presents a peak of sensitivity at the resonance between 20 kHz and 200 kHz. A slight modification of the value of the common mode impedance and/or the impedance to ground will have a predominant effect to shift the resonance frequency of the modification factor and to change its amplitude. The amplitude can be multiplied up to 10 times at the resonant frequency. After this resonance frequency, any changes in the concerned impedances compared to the modeled ones will lead to a proportional change in the modification factor. Before the resonance frequency, the sensitivity values are too low to change the attenuation significantly.

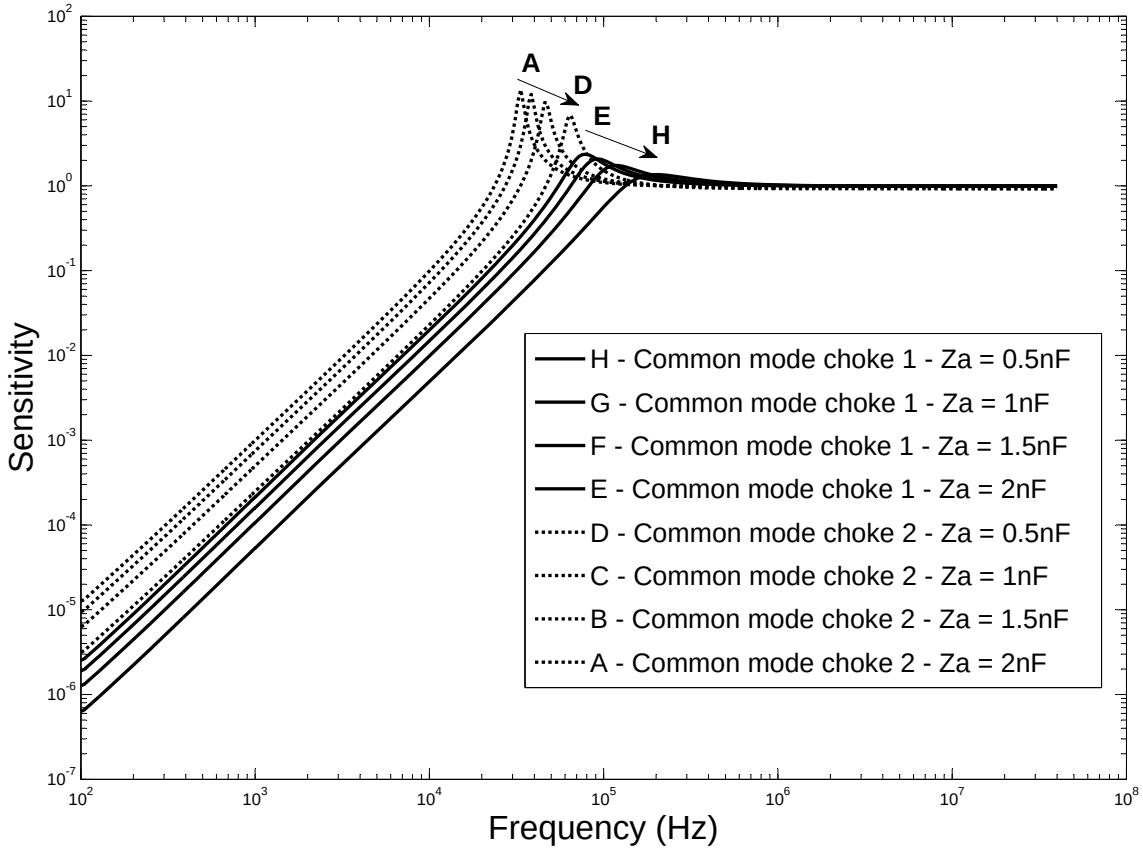

Figure 31: Local sensitivity of the impedance related to the common mode current modification factor.

Deviation

Figure 32 illustrates the upper and lower limits of the modification factor for a tolerance of 10% to 30%. A percentage of error made in the modelling of the impedances is used to evaluate two first upper and lower limits of the modification factors. This percentage has been chosen to be 10% and 30% but can be modified by the user individually for each impedance to precise complex permeability values of a material; or the tolerance of the Y capacitors can then be used to refine the range of incertitude in the modification factors. The second source of deviation is related to the electromagnetic field generated by the cable and hence not included in the measurement.

Designable Parameters: Effect of the Material

The change of material has a main effect to shift the maximum common mode impedance value. The choke is more used for its core loss properties (related to the imaginary part of the complex permeability μ'') and less for its inductive properties (related to the real part of the complex permeability μ'). The main purpose of a common mode choke is not for energy storage but it is for transformation of this energy to heat. Typically the choice of material will depend on the frequency of the noise to be filtered; a material will be efficient if the noise is located in the upper values (above 40%) of μ''.

The change of material is also an alternative when the level of saturation is reached. A nanocrystalline material is for instance a good alternative choice for a saturating choke made of iron.

Designable Parameters: Effect of the Size of the Choke

Fig. **33** presents the effect of the size of the core by comparing the impedances of two common mode chokes with two different sizes: the choke 1 (25×15×5 mm, copper wire thickness) and the choke 1-XL (35×15×7 mm, copper wire thickness 1.5mm). The choke 1 is same as already introduce in the chapter. The choke 1-XL has the same structure but a bigger core.

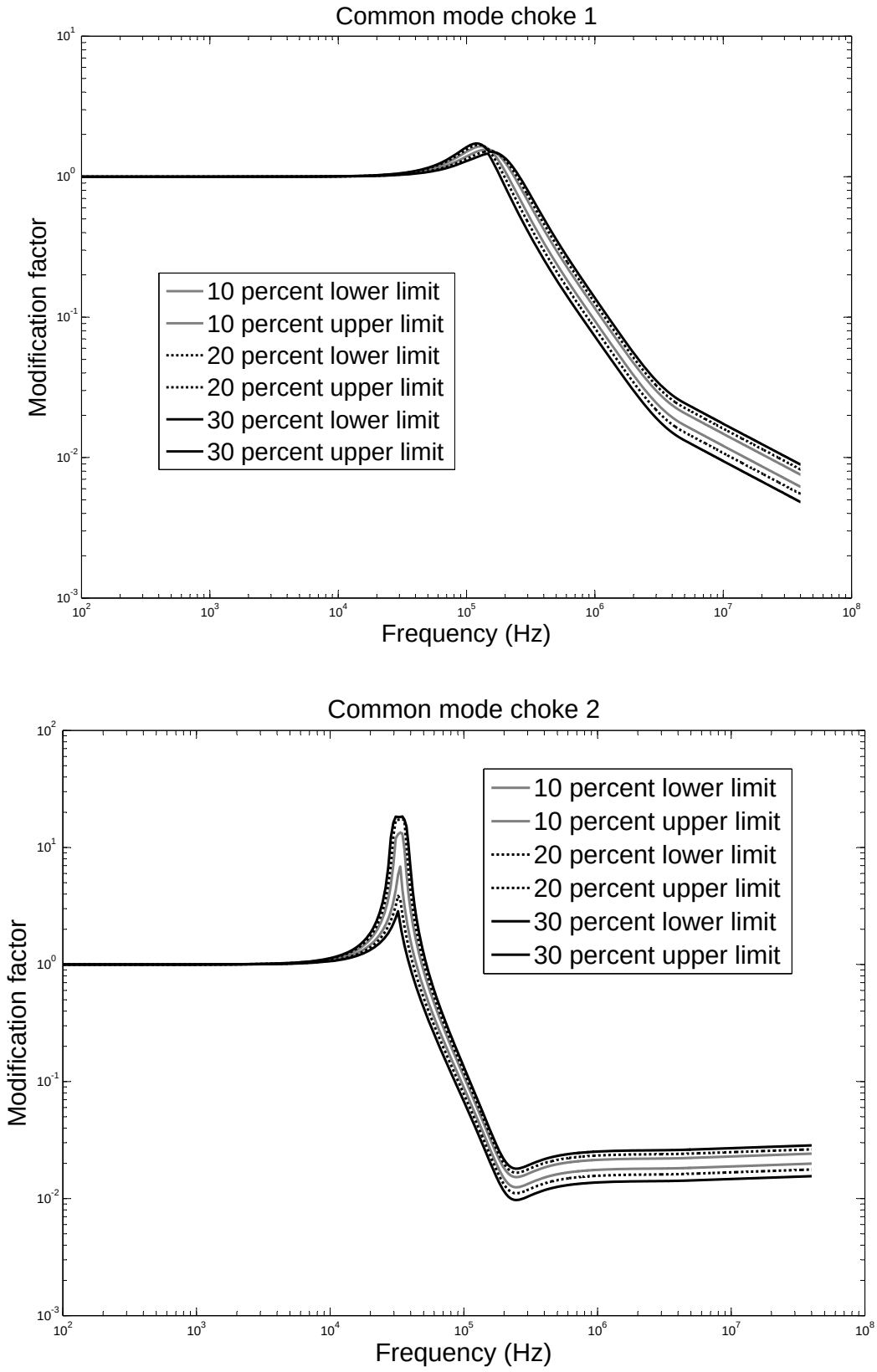

Figure 32: Upper and lower limits of the modification factor (Incertitude from 10 to 30 percent).

The turn to turn capacitance and the leakage inductance of the choke 1-XL are a bit higher due to a thicker and a longer windings but remains within the same range of value.

The increase of the size of the choke tends to shift the maximum value of the common mode impedance towards the lower frequency. This shift may or may not change the frequency at which the attention of the common mode current will start; this frequency is indeed related to the resonance between the impedance to the ground of the system with the common mode impedance. It translates graphically by an intersection of the two respective curves. If this intersection occurs where the common mode impedance is dissimilar between the two chokes, the attenuation of common mode current will then start at a lower frequency for the bigger choke. Else, this frequency remains unchanged.

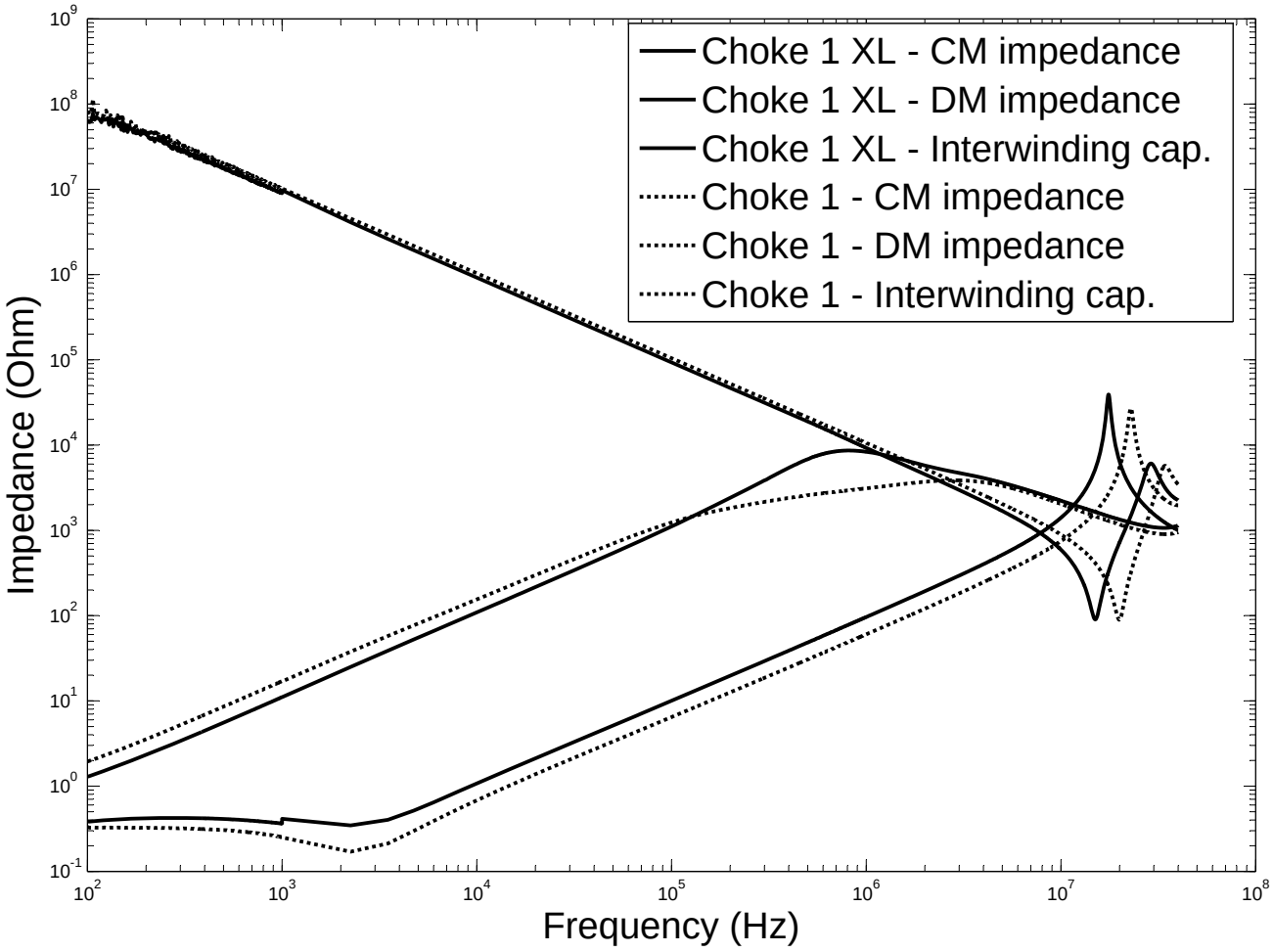

Figure 33: Impedances of two common mode chokes with different core size and same number of turns.

Designable Parameters: Effect of Number of Turns

Fig. **34** shows the influence of the number of turns on the value of the common mode impedances, the phase inductances, the turn to turn capacitances and the differential mode impedances. The core is same for all the four chokes tested.

The value of the common mode impedance increases with the square value of the number of turns. As the real part of the complex permeability is usually higher than its imaginary part, an increase the number of turns will also shift the maximum common mode impedance value towards the lower frequencies. The density of flux in the choke is increased with the number of turn and the saturation level is easier to reach.

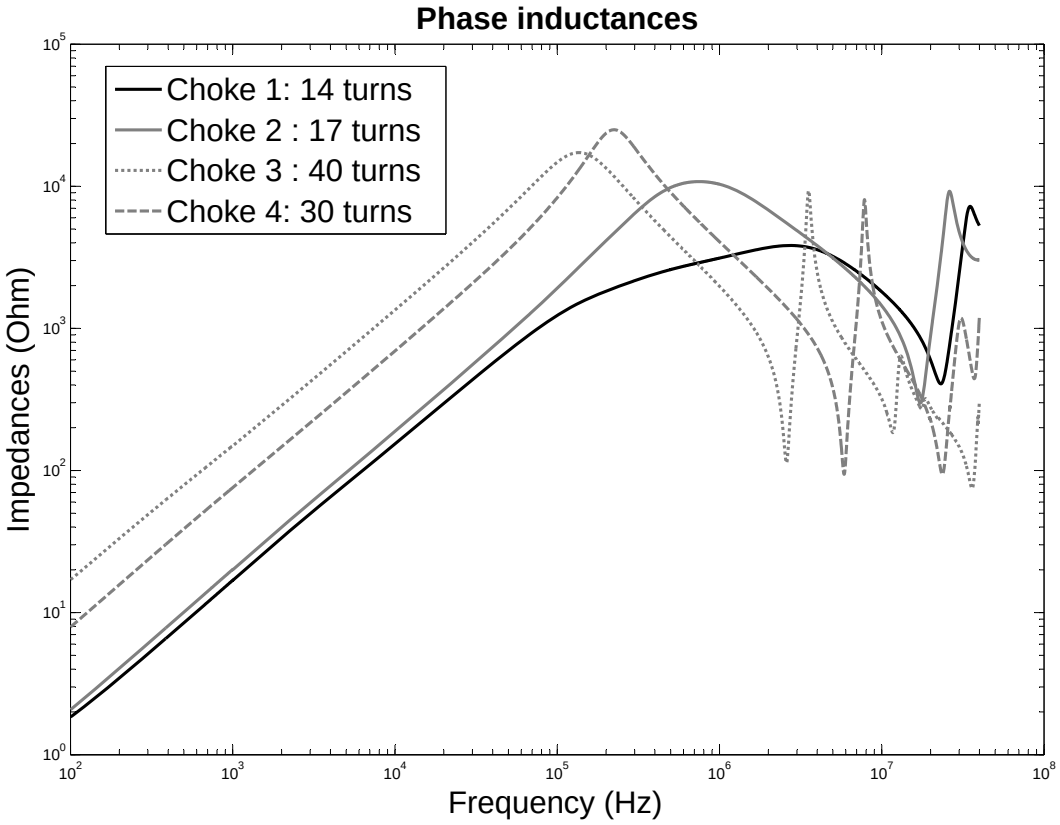
Phase inductances
Choke 1: 14 turns
Choke 2 : 17 turns
Choke 3 : 40 turns
Choke 4: 30 turns
Impedances (Ohm)
Frequency (Hz)

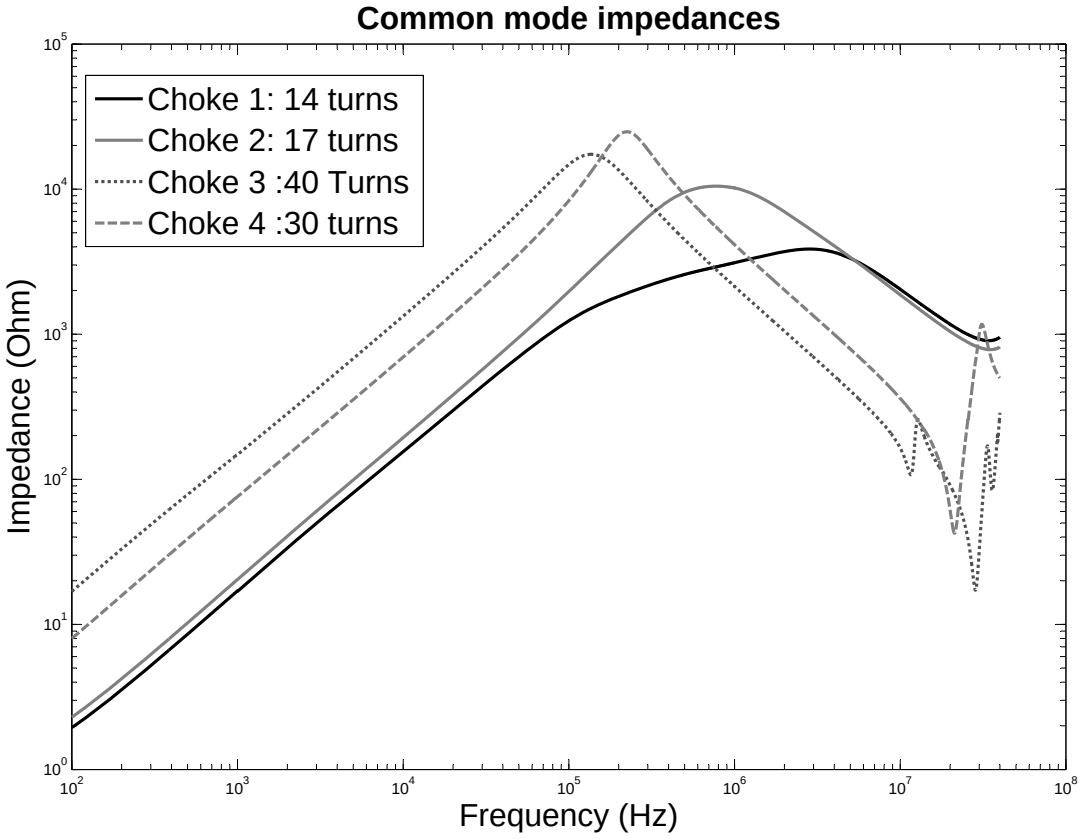
Common mode impedances
Choke 1: 14 turns
Choke 2: 17 turns
Choke 3 :40 Turns
Choke 4 :30 turns
Impedance (Ohm)
Frequency (Hz)

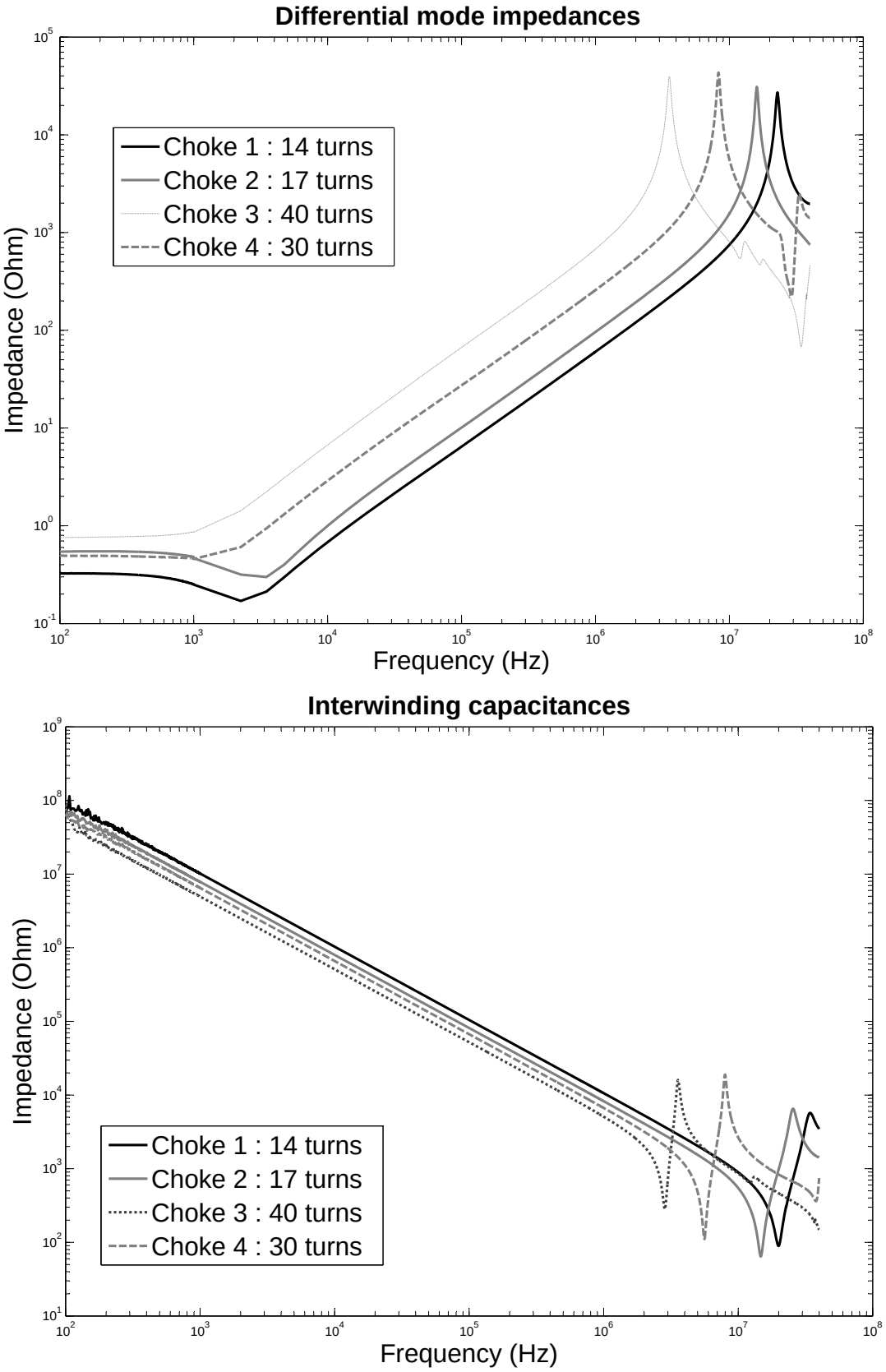

Figure 34: Influence of the number of the number of turns on: common mode impedances, turn to turn capacitances, differential mode impedances.

Designable Parameters: Effect of the Wiring System

Two kinds of windings are possible: the sectional winding and the bifilar winding. Sectional winding consists of the same number of windings placed at diametrically opposite ends on the toroidal core and bifilar winding consists of a parallel wiring around the core. The two families of windings are shown in Fig. **35**. Their respective impedances are presented in Fig. **36**. The main advantage of the sectional winding stands in the high leakage inductance which allows the filtering of the differential mode current in addition of the common mode one. The small leakage inductance provides less attenuation of high frequency differential mode current.

Designable Parameters: Effect of the Wire Dimension

The wire dimension is chosen according to the density of current in the circuit. It has a small effect at very low frequencies where the resistance of the wiring is the main contribution to the impedances. This resistance is visible in the measurement of the leakage inductance at low frequency.

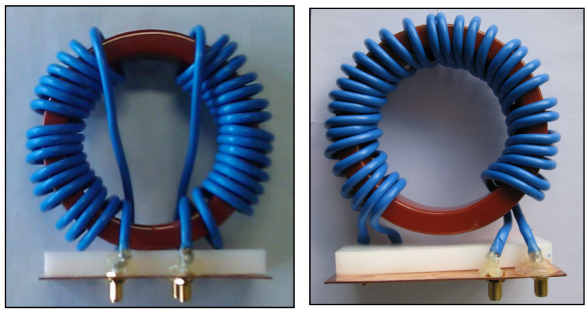

Figure 35: (a) Sectional winding and (b) bifilar winding of a common mode choke.

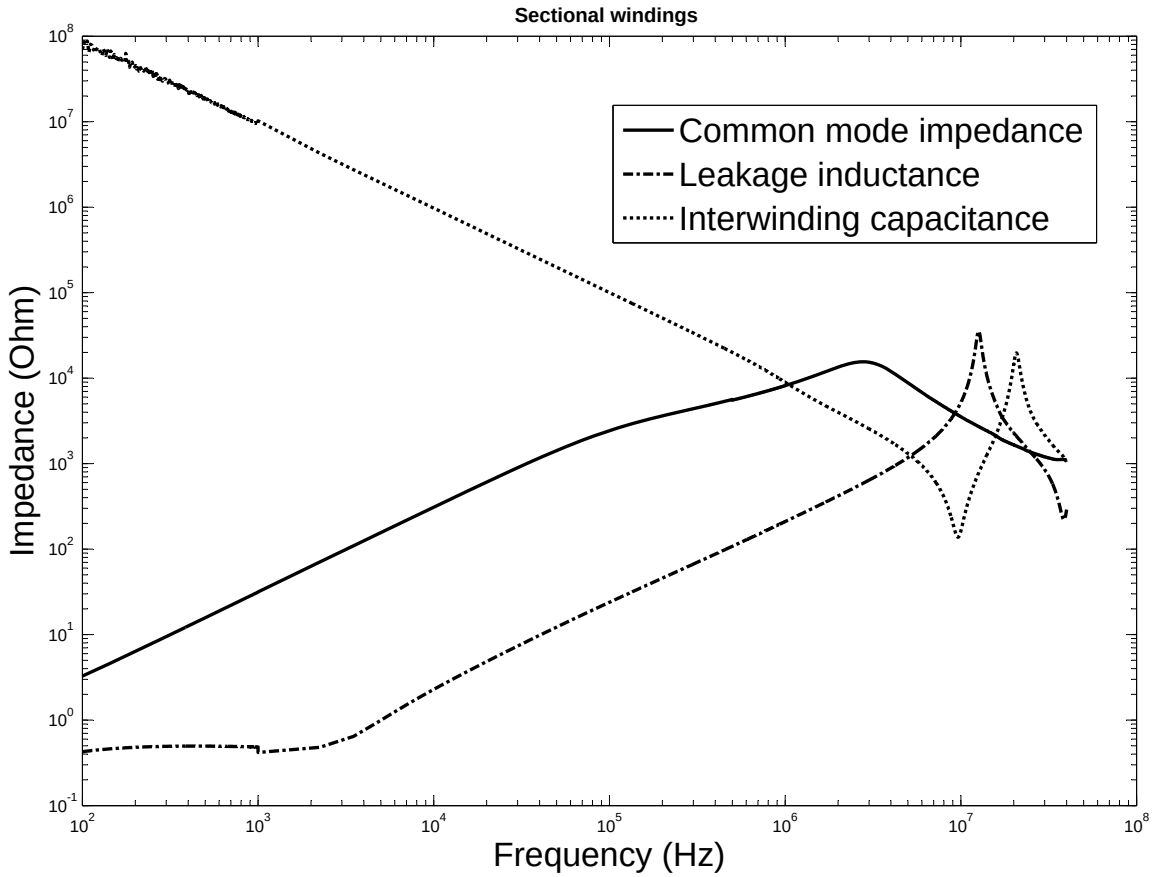

(a) Sectional winding

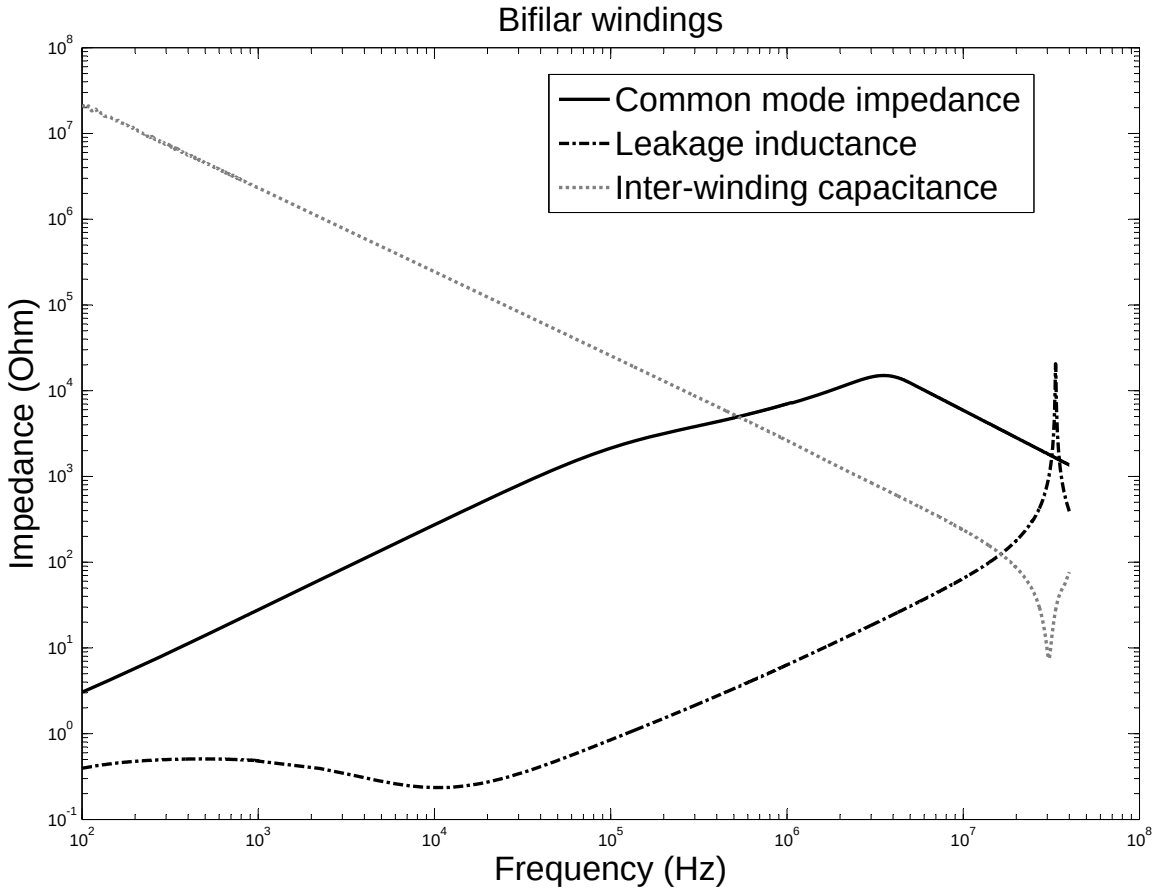

(b) Bifilar windings

Figure 36: Nanocrystalline common mode chokes impedances with different windings.

REFERENCES

[1] Bose, Modern power electronics and AC drives, ISBN 0-13-016743-6, Prentice Hall.

[2] Kempski A, Smolenski R, Kot E, Fedyczak Z. Active and passive series compensation of common mode voltage in adjustable speed drive system, Industry Applications Conference, 2004. 39th IAS Annual Meeting. Conference Record of the 2004 IEEE, 2004; 4: pp. 2665-2671.

[3] Roc'h A, Bergsma H, Leferink FBJ, Zhao D, Polinder H, Ferreira JA. Design of an EMI Output Filter For Frequency Converters, in Proc. EMC Europe International Symposium on EMC, Barcelona, Spain, 2006.

[4] Frank Leferink, Hans Bergsma, Braham Ferreira, Wim van Etten. High Performance EMI Filter for Frequency Converters, EMC Europe 2004, Eindhoven.

[5] 'Introduction to electromagnetic compatibility' Clayton R. Paul, ISBN 978-0-471-75500.

[6] EMI Self-Learning Toolkit for Switched-Mode Power Supply, AUNP program, http://www.kmitl.ac.th/emc/emitoolkit.htm

[7] Massarini A, Kazimierczuk MK. Self-capacitance of inductors. IEEE Trans Power Electron 1997; 12(4): 671-676.

[8] Grandii G, Kazimiercmk Massarini A. Lumped. Parameter for models for single- and Multiple-layer Inductor, IEEE PESC '96.

[9] Agilent technologies Impedance measurement handbook July 2006, www.agilent.com

[10] Fairites, Technical Information, How to choose Ferrite Components for EMI suppression, www.fair-rite.com

[11] Takanori T. Frequency dispersion of complex permeability in Mn-Zn and Ni-Zn spinel ferrites and their composite materials. J Appl Phys 2003; 93(5): 2789-2796.

[12] Nave MJ, Technol Sverdrup, AL Huntsville. On modeling the common mode inductor Electromagnetic Compatibility, 1991. Symposium Record. IEEE 1991 International Symposium on, 12-16 Aug 1991; 452-457.

[13] Margarita D. Takach, Peter O. Lauritzen: Survey of Magnetic Core Models, IEEE APEC Record, 1995; pp. 560-566.

[14] Jiles DC. Atherton DL. Theory of ferromagnetic hysteresis. J Magn Magn Mater 1986; 61: 48-56.

[15] NL Mi, Oruganti R, SX Chen. Modeling of hysteresis loops of ferrite cores excited by a transient magnetic field Magnetics, IEEE Trans 1998; 34(4): 1294-1296

[16] Jiles DC. Frequency dependence of hysteresis curves in 'non-conducting' magnetic materials, Magnetics. IEEE Trans; 1993; 29(6): 3490-3492.

[17] Izydorczyk J. Magnetics IEEE Trans 2006; 42(10): 3132–3134.

[18] Saltelli T, Campolongo R. Sensitivity Analysis in Practice_ A Guide to Assessing Scientific Models, 2004.

[19] Vlach, Singhal, Computer methods for circuit analysis and design, 1983, ISBN 978-0442011949.

[20] Vacuumschmelze Gmbh&Co KG, Technical Information, Nanocrystalline material in common mode chokes.

[21] Magnetics, Technical Information. A Critical Comparison of Ferrites with Other Magnetic Materials, www.mag-inc.com

[22] Handbook of Magnetic Material, vol. 1, 2 and 6.ISBN: 0-444-51459-7.

[23] Handbook of modern ferromagnetic material, Alex Goldman. ISBN: 0-412-14661-4.

[24] Inductive components and appropriate magnetic materials for filters in SMPS-designs; Wanior, J, Industrial Technology, 2003 IEEE International Conference on Volume 2, 10-12 Dec. 2003, Vol. 2, pp.1178–1183.

[25] Fe-M-B nanocrystalline soft magnetic materials: a review of soft magnetic material development, Kiyonori Suzuki, Properties and application of Nanocrystalline alloys form amorphous precursors.

[26] Switched mode power supply handbook, Billings, Keith, H., ISBN 0-07-005330-8.

[27] Electric Motors and Drives, Austin Hughes, ISBN-13: 978-0-7506-4718-2.